

1 **Title: Four meromictic (?) lakes in Itasca State Park, Minnesota,**
2 **U.S.A.**

3 Authors: Elizabeth D. Swanner^{1*} (eswanner@iastate.edu), Chris Harding¹
4 (charding@iastate.edu), Sajjad A. Akam¹ (sajjad@iastate.edu), Ioan Lascu² (lascul@si.edu),
5 Gabrielle Ledesma^{1,3} (gmledesma@mun.ca), Pratik Poudel^{1,4} (poudelp@iastate.edu), Heeyeon
6 Sun^{1,4} (heeyeons@iastate.edu), Samuel Duncanson^{1,4} (sdunc@iastate.edu), Karly Bandy⁴
7 (kbandy14@iastate.edu), Alex Branham⁴ (abranham@iastate.edu), Liza Bryant-Tapper⁴
8 (ebtapper@iastate.edu), Tanner Conwell⁴ (tconwell@iastate.edu), Omri Jamison⁴
9 (shaylinj@iastate.edu), and Lauren Netz⁴ (lenetz@iastate.edu).

10

11 Affiliations:

12 ¹Department of Geological & Atmospheric Sciences, Iowa State University, Ames, IA, 50010,
13 USA

14 ²Department of Mineral Sciences, National Museum of Natural History, Smithsonian Institution,
15 Washington, DC, 20560, USA

16 ³Department of Earth Sciences, Memorial University of Newfoundland, St. John's, Canada

17 ⁴Students in GEOL 406/506, Spring 2022, Iowa State University, Ames, IA, 50010, USA

18

19 *Corresponding Author: 2237 Osborn Drive, 253 Science Hall, Ames, IA 50010, USA;

20 eswanner@iastate.edu

21

22 This paper is a non-peer reviewed preprint submitted to EarthArXiv. The preprint has also been
23 submitted to *Limnology and Oceanography*.

24
25 Author Contributions: Individuals in parenthesis contributed substantially to the study's
26 conception (EDS), data acquisition (EDS, CH, SAA, IL, GL, PP, HS, SD, KB, AB, LB-T, TC,
27 OJ, LN), or analysis (EDS, CH, SAA, GL, PP, HS, SD, KB, AB, LB-T, TC, OJ, LN);
28 contributed substantially to drafting the manuscript (EDS, CH, SAA, GL, PP, HS, SD, KB, AB,
29 LB-T, TC, OJ, LN); and approved the final submitted manuscript (EDS, CH, SAA, IL, GL, PP,
30 HS, SD, KB, AB, LB-T, TC, OJ, LN).

31
32 Keywords: meromictic, chemocline, subsurface chlorophyll maximum, subsurface oxygen
33 maximum

34 **Abstract**

35 Four adjacent lakes (Arco, Budd, Deming, and Josephine) within Itasca State Park in Minnesota,
36 USA are reported to be meromictic in the scientific literature. However, seasonally persistent
37 chemoclines have never been documented. We collected seasonal profiles of temperature and
38 specific conductance and placed temperature sensor chains in two lakes for ~ 1 year to explore
39 whether these lakes remain stratified through seasonal mixing events, and what factors contribute
40 to their stability. The results indicate that all lakes are predominantly thermally stratified and are
41 prone to mixing in isothermal periods during spring and fall. Despite brief, semi-annual erosion
42 of thermal stratification, Deming Lake showed no signs of complete mixing from 2006 to 2009
43 and 2019-2022. Geochemical data indicate that water in Budd Lake, the most dilute lake, is
44 predominantly sourced from precipitation. The water in the other three lakes is calcium-
45 magnesium bicarbonate type, reflecting a source of water that has interacted with the landscape.
46 $\delta^{18}\text{O}_{\text{H}_2\text{O}}$ and $\delta^2\text{H}_{\text{H}_2\text{O}}$ measurements indicate the lakes are supplied by precipitation modified by

47 evaporation. The water residence time in meromictic Deming Lake is short (100 days), yet it
48 maintains a large reservoir of dissolved iron. Josephine, Arco, and Deming lakes sit in a valley
49 with likely permeable sediments and may be hydrologically connected through wetlands, and
50 recharged with shallow groundwater, as no streams are present. All four lakes develop
51 subsurface chlorophyll maxima layers during the summer. All lakes also develop subsurface
52 oxygen maxima that may results from oxygen trapping in the spring by rapidly developed
53 thermoclines.

54 **Introduction**

55 Meromictic lakes, which do not mix seasonally, maintain anoxic bottom waters that
56 minimize sediment resuspension and bioturbation and permit the development of laminated or
57 varved sediments (Anderson et al. 1985; Anderson and Dean 1988). Such sediments can record
58 climatic transitions, vegetation changes, changes in sediment transport, and atmospheric
59 deposition patterns (O’Sullivan 1983). Laminated sediments are also useful for studying the
60 formation, deposition, and diagenetic transformation of chemically precipitated minerals
61 (Wittkop et al. 2020; Ledesma et al. 2022). Such sediments are useful to interpret the origin of
62 minerals in sediments deposited from past stratified marine waters when such conditions no
63 longer exist (Degens and Stoffers 1976; Swanner et al. 2020). Meromictic lakes are present on all
64 continents but are thought to be rare (Walker and Likens 1975; Stewart et al. 2009; Hall and
65 Northcote 2012).

66 Lakes can develop meromixis when surface wind action does not mix the epilimnion, the
67 upper layer of the lake, with the monimolimnion, the deepest layer of the lake. Meromictic lakes
68 are characterized by a sharp increase in electrical conductivity at a chemocline separating a cold
69 and/or dense monimolimnion from the epilimnion (Boehrer and Schultze 2008). The epilimnion

70 is in contact with the atmosphere, while the monimolimnion is anoxic. This results in changing
 71 sedimentation patterns compared to lakes that mix regularly. A sediment indicator of an anoxic
 72 monimolimnion typical of low sulfur meromictic lakes is enhanced burial of oxygen-sensitive
 73 mineral forming elements, particularly iron and manganese (Dean and Schwalb 2002; Wittkop et
 74 al. 2014).

75 Lake morphometry is a key factor in the development of meromixis. Lakes that are
 76 relatively deep compared to their surface area, which determines the fetch upon which wind can
 77 act, are less likely to overturn (Wetzel 2001). The potential for water column stratification is
 78 reflected by relative depth (Z_r), which is the ratio of the maximum lake depth (Z_m) to the
 79 diameter of a circle of area equal to that of the lake (A^0), expressed as a percentage.

$$80 \quad Z_r (\%) = \frac{Z_m}{2} \sqrt{\frac{\pi}{A_0}} \times 100 \quad (1)$$

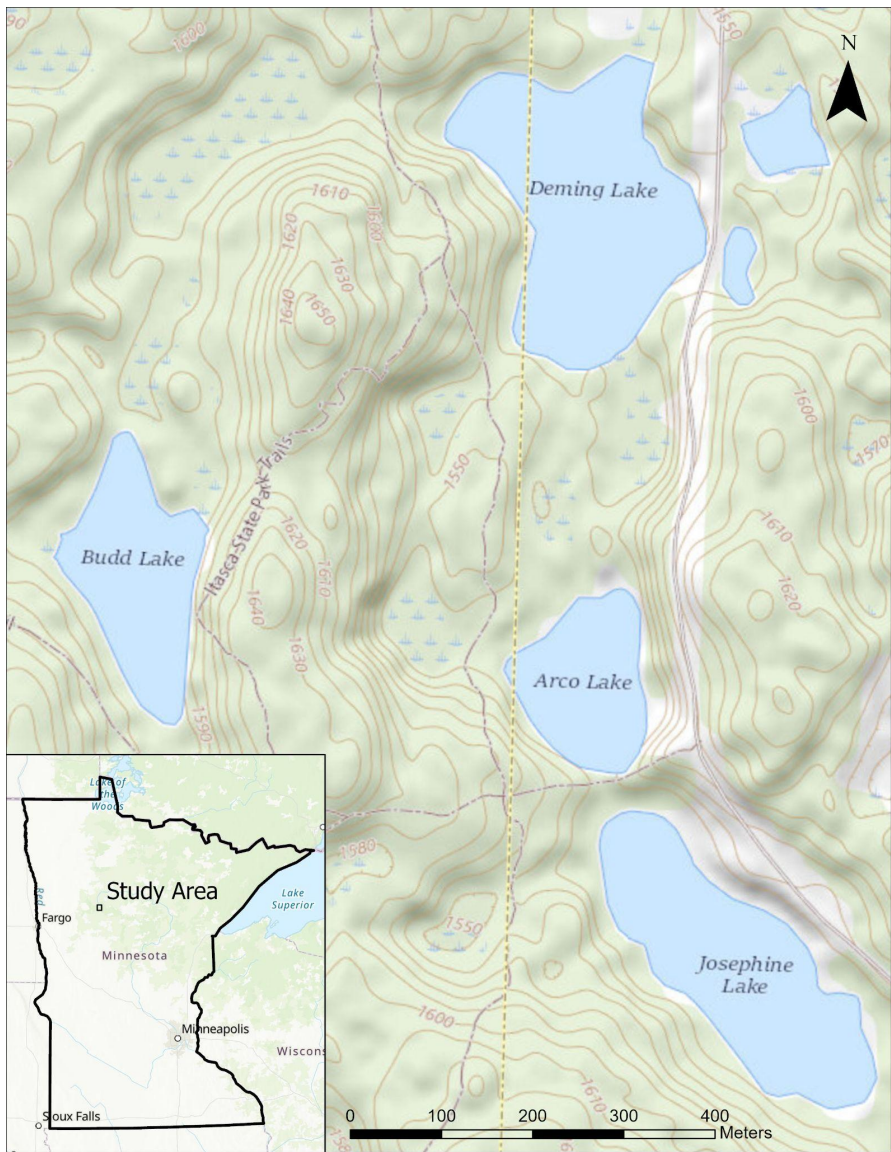
81 Most temperate zone lakes prone to meromixis have relative depths exceeding 4% and A^0 of less
 82 than 0.5 km² (Swanner et al. 2020). Meromixis can also result from increased chemical
 83 constituents that enrich the water density of monimolimnion, such as from runoff, groundwater
 84 inputs, and remineralization processes associated with organic carbon loading (Hakala 2004;
 85 Schultze et al. 2017). The identity of the substances causing increased density varies depending
 86 on the catchment characteristics but can include dissolved iron and manganese, as well as
 87 dissolved inorganic carbon (Kjensmo 1967; Hongve 2002).

88 Gradients of dissolved oxygen and inorganic nutrients are mediated by primary
 89 productivity and uptake in the epilimnion and sinking and decomposition of biomass in the
 90 monimolimnion (Camacho 2006). Stratification limits the return of nutrients to the epilimnion. A
 91 subsurface chlorophyll maximum layer (SCML) often develops within the metalimnion, the
 92 middle seasonally mixed layer of meromictic lakes (Baker and Brook 1971; Camacho 2006).

93 Stable stratification, the availability of both light and nutrients, and zooplankton grazing drive
94 the formation and location of the SCML in meromictic lakes (Klausmeier and Litchman 2001;
95 Pilati and Wurtsbaugh 2003). Primary productivity is often highest within the SCML (Camacho
96 2006).

97 Four lakes in Itasca State Park, Minnesota, USA - Arco, Budd, Deming, and Josephine
98 (Figure 1) - have been described as meromictic in the scientific literature since the 1960s (Baker
99 and Brook 1971; Anderson et al. 1985; Stewart et al. 2009). However, there has never been
100 physical and chemical data from all lakes during all seasons - especially spring and fall when
101 mixing would be expected - to document through the maintenance of a chemocline that they are
102 meromictic. The goals of this study are to 1) determine whether these four lakes are meromictic,
103 2) investigate the water type, sources, and reasons for meromixis, and 3) describe the unique
104 biological features of these lakes. To achieve these goals, we conducted fieldwork from 2006-
105 2009 and 2019-2022, and integrated data from University of Minnesota students working at the
106 Itasca Biological Station and Laboratories since the 1950s. We hope that this description of the
107 lakes will spur new investigations that utilize their unique geomorphological and biogeochemical
108 features.

109 **Methods**



110
111 Figure 1: Map of the four study lakes within Itasca State Park, Minnesota.

112
113 Formation of the four study lakes occurred during the late-Wisconsin glaciation ~12,000
114 years ago (marine isotope stage 2; Jennings and Johnson 2011). They occupy a tunnel valley that
115 was formed beneath the Wadena lobe of the Laurentide Ice Sheet. Following glacial retreat, the

116 melting of stagnant ice blocks within the tunnel valley left depressions in the landscape now
117 occupied by lakes and wetlands (Wright Jr. 1993).

118 Today, the four lakes investigated in this study sit in the HUC-12 watershed that sources
119 the headwaters of the Mississippi River (U.S. Geological Survey 2017). Budd (478.6 meters
120 above mean sea level; MAMSL) is the highest elevation, while Arco (465.8 MAMSL) and
121 Josephine (465.4 MAMSL) lie at similar elevations. Deming is the lowest elevation of the lakes
122 (464.8 MAMSL).

123 Lake depth measurements were collected using a Garmin Striker 4 dual-beam transducer
124 (sonar) attached to a rowboat or canoe. Depth and GPS measurements were taken every six
125 seconds while the boat was in motion. A Garmin GLO 2 GPS receiver and ArcGIS Collector app
126 was used to navigate, track the boat's course, and ensure even coverage. The shoreline of the
127 lakes was obtained by walking along accessible areas of the shore with the Garmin GLO 2 GPS
128 receiver, or from Lidar-derived digital elevation models. Bathymetry rasters (1 m resolution)
129 were generated from the depth measurements in ArcGIS Pro 3.0 using a 3rd-degree Local
130 Polynomial Interpolation. These rasters were used to calculate lake volumes and contour maps.
131 Rasters and volume data have been deposited with the Environmental Data Initiative (Swanner et
132 al. 2022).

133 Chemical, physical, and biological parameters measured on the four lakes included depth,
134 temperature, specific conductance, salinity, turbidity, pH, oxidation-reduction potential,
135 dissolved oxygen, photosynthetically active radiation, chlorophyll-a, and phycocyanin. Major
136 cations, anions, and isotopes of water ($\delta^2\text{H-H}_2\text{O}$ and $\delta^{18}\text{O-H}_2\text{O}$) were determined on lake water
137 retrieved from different depths within the four lakes. Taxon-specific chlorophyll-a fluorescence

138 was collected with a Fluoroporbe (BBE Moldaenke). The data and description of methods are
139 available in the Environmental Data Initiative (Swanner et al. 2022).

140 A string of temperature loggers (HOBO Water Temp Pro v2) placed at different depths
141 were deployed into the deep areas of Deming, Arco, and Budd lakes for one year. A conductance
142 logger (HOBO Conductivity Logger) was added near the bottom of the strings in Arco and Budd
143 after six months. These sensors measured temperature every thirty minutes and specific
144 conductivity every 2 hours. The sensor string was not retrieved from Budd, as it could not be
145 located. Conductance measurements with a Yellow Spring Instruments ProDSS
146 temperature/conductivity sensor on deployment and removal were used to check for drift in the
147 HOBO conductance logger. Hourly wind speed data for the duration of sensor deployment
148 utilized the ITCM5 weather station in Itasca State Park. Data was downloaded from MesoWest
149 (<https://mesowest.utah.edu/>). Plots and analyses were produced in Python or R Studio
150 (2022.07.2) using the RLakeAnalyzer package v.1.11.4.1 (Winslow et al. 2019).

151 Major anions (CO_3^{2-} , HCO_3^- , Cl^- , and SO_4^{2-}) and cations (Na^+ , K^+ , Ca^{2+} , Mg^{2+}) were used
152 to produce a Piper diagram in Geochemist's Workbench 15.0. The concentration of cations and
153 anions was calculated as the percentage of total cations and anions in meq L^{-1} .

154 The isotopes of water ($\delta^2\text{H}_{\text{H}_2\text{O}}$ and $\delta^{18}\text{O}_{\text{H}_2\text{O}}$) were measured on spring or seep water that
155 had been filtered with 0.45 micron nylon syringe filters and stored at 4 °C with minimal
156 headspace until analysis. Samples were analyzed with a Picarro L1102-i Isotopic Liquid Water
157 Analyzer at the Stable Isotope Laboratory at Iowa State University. The analytical uncertainty
158 and average correction factor for $\delta^{18}\text{O}_{\text{H}_2\text{O}}$ are ± 0.05 ‰ and ± 0.30 ‰ for $\delta^2\text{H}_{\text{H}_2\text{O}}$ relative to V-
159 SMOW.

160 Samples for microscopy and water color were collected into amber bottles with a Van
 161 Dorn sampler from three different depths in each lake, including the SCML, if present, as
 162 determined with the YSI ProDSS. Water color was determined on water filtered through a GF-75
 163 (Advantec) glass fiber filter (Cuthbert and del Giorgio 1992). Absorbance was measured at 440
 164 nm and 750 nm. The absorbance at 750 nm was subtracted from the absorbance at 440 nm. The
 165 absorption coefficient was calculated with the equation:

$$166 \quad g \text{ (m}^{-1}\text{)} = (2.303 * \text{Absorbance}) / (\text{path length}) \quad (2)$$

167 A conversion was necessary to determine the color of the lake water as seen below.

$$168 \quad \text{Color (mg Pt L}^{-1}\text{)} \text{ } g_{440} \text{ (m}^{-1}\text{)} = 18.216 * [g_{440} \text{ (m}^{-1}\text{)}] - 0.209 \quad (3)$$

169 Water sampled from the SCML was preserved with 1% Lugol's solution upon returning
 170 to the lab. Fixed samples were settled in the dark for three to seven days.

171 Student reports from courses taking place over several decades at the Itasca Biological
 172 Station and Laboratories (IBSL) (Knoll and Cotner 2018), formerly the Itasca Biological Station,
 173 were acquired from the library at the University of Minnesota, Twin Cities.

174 **Results & Discussion**

175 Table 1. Morphometric parameters for the four study lakes.

Lake	Volume (m^3)	Surface Area (m^2)	Maximum Depth (m)	Relative Depth (%)	Fetch Distance (m)	Fetch Heading (degrees)
Arco	142,628.73 m^3	24180 m^2	12.6 m	7.3%	210.4 m	175 deg.
Budd	183,441.22 m^3	28184.5 m^2	16.1 m	8.8%	310.3 m	169 deg.
Deming	242,701.12 m^3	54325 m^2	20.8 m	7.3%	346.7 m	188 deg.
Josephine	315,765.05 m^3	52711 m^2	14.5 m	5.7%	432.4 m	136 deg.

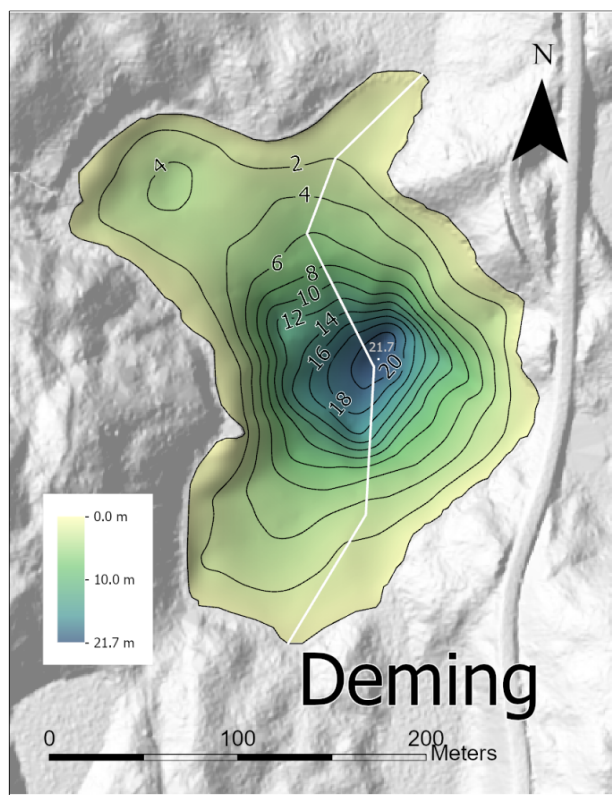
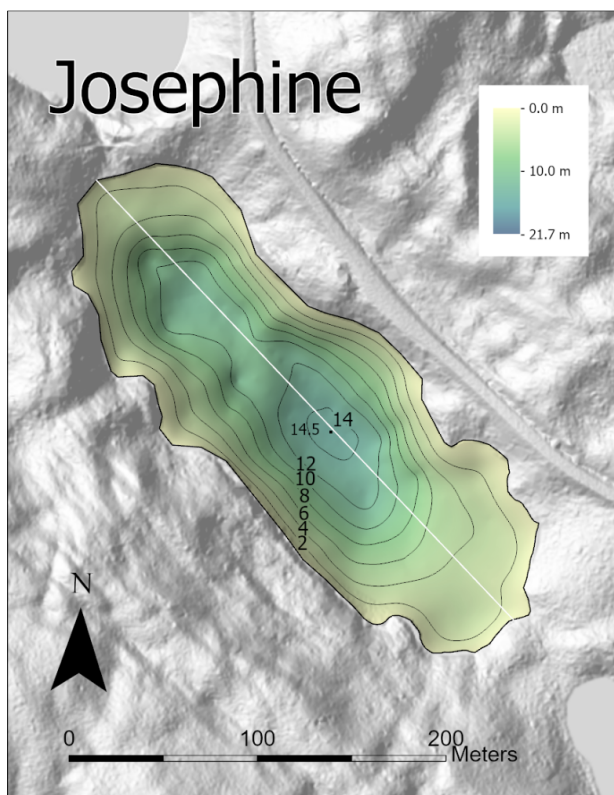
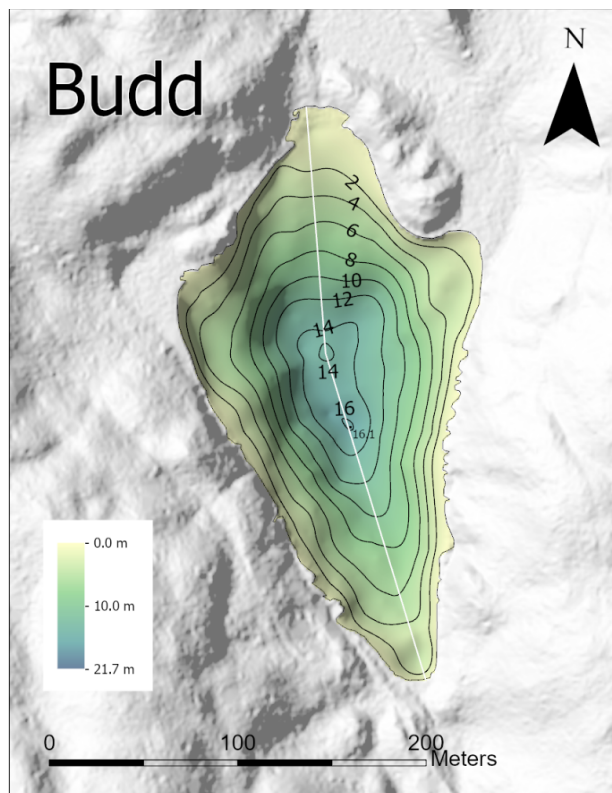
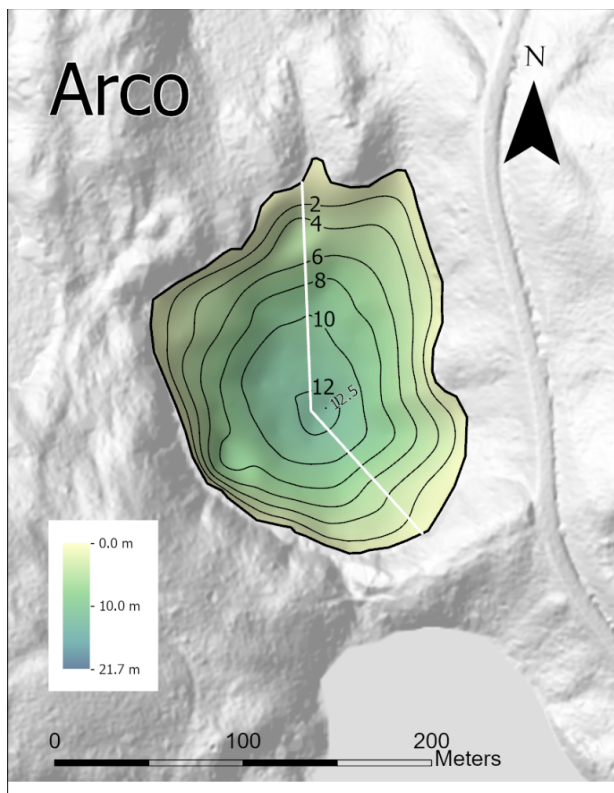
176

177 *Morphometry and Mixing Status*

178 Deming is the largest and deepest of the four study lakes with a 54,325 m² surface area
179 and a maximum depth of 20.8 meters (Table 1). The maximum depth of Deming Lake has
180 previously been reported as 16.5 m (Hooper 1951), 17 m (Baker and Brook 1971), and 17.6 m
181 (Lascu and Plank 2013). Differences in technology and the small surface area (4.3%) with water
182 depths at or below 17 m could account for the variation. Long-term water-level fluctuations may
183 be induced by drought (Lascu et al. 2012). In all lakes, steep-sided deep holes were detected
184 (Figure 2). It is possible that temperature, pressure, and/or salinity gradients present at the tops of
185 these holes could deflect sound beams, causing errors in our depth measurements (Boehrer and
186 Schultze 2008). These factors could have affected all lakes, which were found to be
187 systematically deeper than previously reported.

188 Josephine has the longest fetch and lowest Z_r of all study lakes. The maximum depth of
189 Josephine Lake (14.8 m) has previously been reported as 10.3 m (Baker and Brook 1971), 12-13
190 m (Callis et al. 1976), and 13 m (Gage and Gorham 1985). The surface area with depths at or
191 below 13 m in Josephine Lake is 5.1%. There was the greatest variation between the previously
192 reported maximum depth of Budd Lake (10.8 m; Baker and Brook 1971) and ours (16.1 m).
193 Budd Lake has the highest Z_r (8.8%). Arco Lake has the smallest surface area of 24,180 m² and a
194 maximum depth of 12.8 m. Arco and Budd Lakes have steep banks along their eastern sides
195 (Figure 1). All lakes exceed a Z_r of 4% and have surface areas of less than 500,000 m², typical of
196 meromictic lakes in the temperate zone (Swanner et al. 2020).

197



199 Figure 2. Bathymetric maps of the study lakes overlain on the digital elevation models. Depth is
200 in meters. The fence diagrams correspond to the cross-sections in Supplementary Figure 1.

201
202 Deming Lake has the longest record of seasonal profiles (2006-2009 and 2019-2022), as
203 its sediments have previously been used to investigate Holocene climate variations (Lascu et al.
204 2012; McLauchlan et al. 2013). A chemocline, or sharp increase in specific conductance, persists
205 in Deming Lake at all sampled times (Figure 3), which is expected for a meromictic lake. The
206 chemocline occurs at 11-13 m (Figure 3). The chemocline was below 10 m in 1989 (Church et
207 al. 1989), and from 11-13 m a decade later (Reiter et al. 1998) based on temperature-
208 compensated conductance measurements from IBSL student reports, indicating that the
209 chemocline has been at a consistent depth for decades. Earlier observations from numerous
210 student reports indicate a much shallower chemocline in Deming Lake, below 5 m (Engstrom et
211 al. 1974; Karli and Keller 1975; Habedank 1990; Bieter et al. 1991; Condon et al. 1996; Nelson
212 et al. 2011). Many of these measurements were made as conductivity without a standardized cell
213 geometry and may or may not have been corrected to a temperature of 25°C, which is necessary
214 for comparing samples across the thermocline. The temperature-compensated and specific cell
215 geometry measurements in our dataset (i.e., specific conductance) likely better capture the
216 variation in dissolved ions comprising the chemocline.

217 A systematic increase in the magnitude of specific conductance readings below the
218 chemocline was observed from the 2006-2009 to the 2019-2022 datasets (Figure 3). This could
219 either be an artifact of instrumentation and calibration differences between the two datasets or
220 could represent a temporal change in water column properties. The counties encompassing Itasca
221 State Park experienced extreme drought for several months in the spring of 2006 and exceptional

222 drought for a few weeks in the summer of 2021(National Oceanographic and Atmospheric
223 Administration; Supplementary Figures 2 and 3). This could have increased the lake's salinity
224 through increased evaporation (Jellison and Melack 1993). Alternatively, or in addition, the
225 magnitude of water sources of differing salinities may have been altered (Ludlam and Duval
226 2001). In the second case, a drought would decrease the magnitude of low specific conductance
227 precipitation and increase the proportion of higher specific conductance groundwater to the
228 annual water budget. As Deming Lake does not have a surface inlet, changes in streamflow can
229 be neglected. The period from 2006-2009 was generally dry, and the amount of recharge to the
230 groundwater system may have also decreased over a multi-year period, effectively decreasing
231 groundwater inputs to the lake, and counteracting the effects of evaporation on specific
232 conductance in Deming Lake. In 2019-2022, the exceptional drought was short-lived and
233 specific conductance might better reflect decreases in precipitation than decreases in recharge,
234 resulting in greater specific conductance values. Another possibility is that variations in the
235 amount of in-lake primary productivity could modulate the specific conductance in the
236 monimolimnion (Campbell 1977). Finally, a longer time since a mixing event could also increase
237 the dissolved solute load from 2019-2022 relative to 2006-2009 (Katsev et al. 2010).

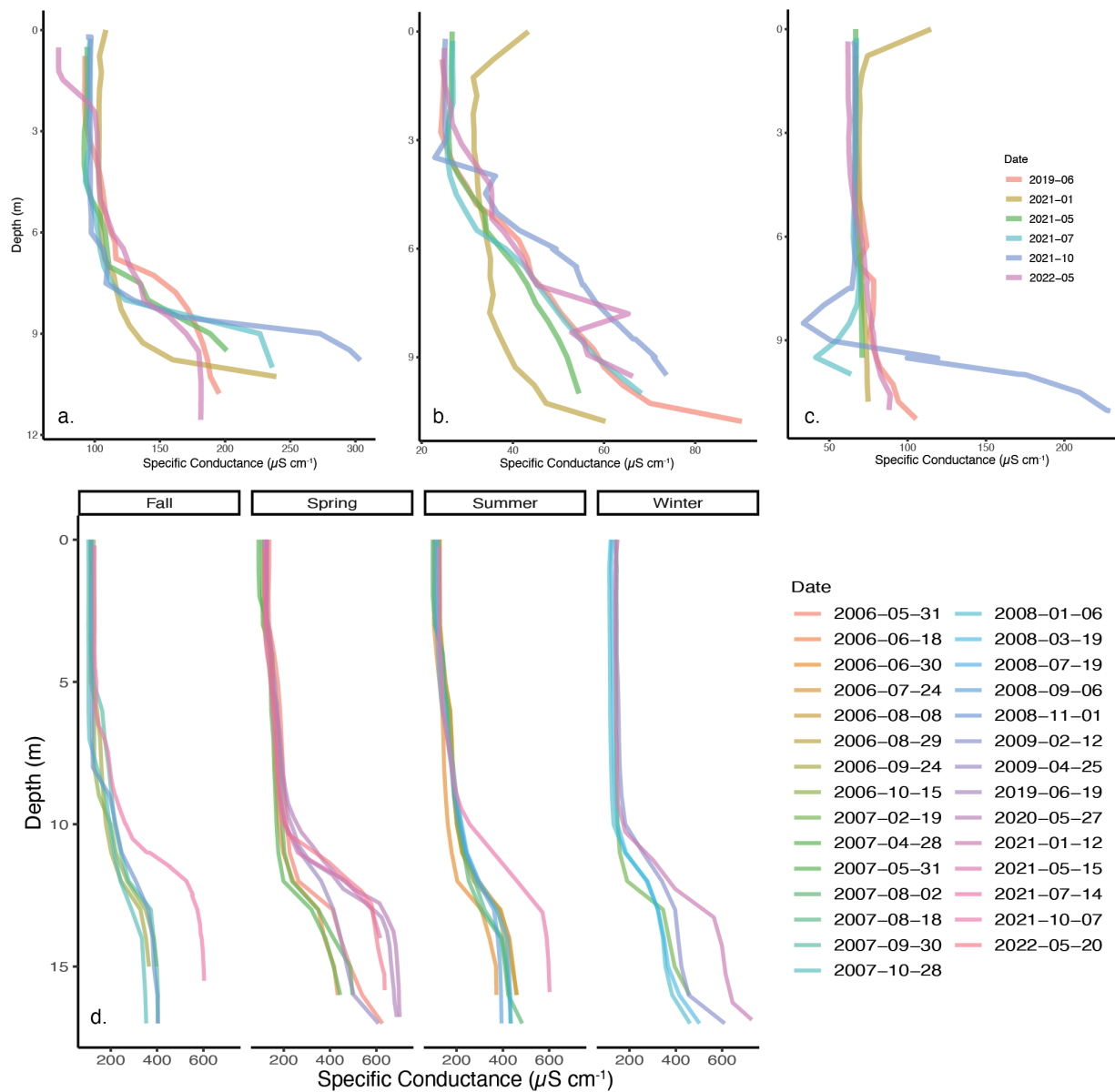
238 A chemocline was present at all time points for Arco Lake between 7-10 m except for
239 May 2022 (Figure 3). It was poorly developed in May 2021, and its deepest occurrence was in
240 January 2021. Arco Lake has a maximum depth of 12.8 m, but no specific conductance data was
241 collected below 12 m as part of the profiles acquired during the study period due to the difficulty
242 of finding the small deep spot (1.7% of surface area). The chemocline is shallowest in mid-
243 summer, consistent with the 7 m chemocline observed in temperature-equilibrated conductivity

244 readings in 1975 and 1976 (Evans and Bjerklie 1975; Barnes et al. 1976), and 2011 (Harren et al.
245 2011).

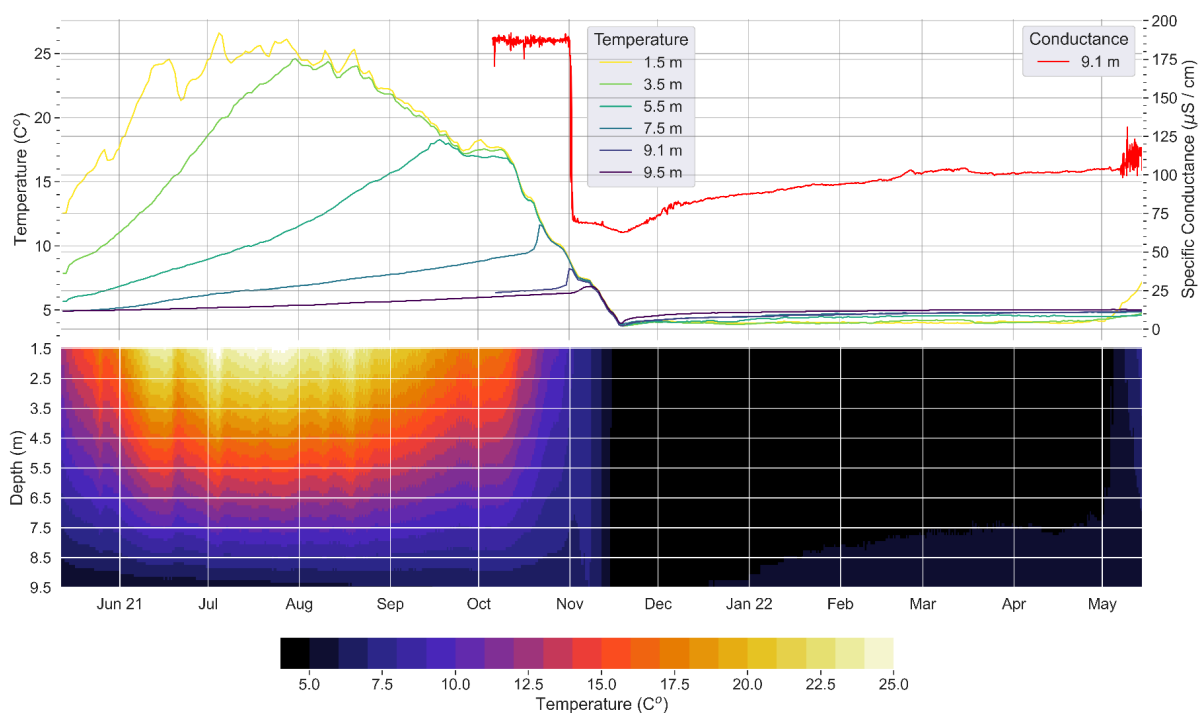
246 Budd Lake had the lowest range of specific conductivity values (23-90 $\mu\text{S cm}^{-1}$). A
247 weakly demarcated chemocline was observed around 4-5.5 m water depths for May 2021, July
248 2021, October 2021, and May 2022. The January 2021 profile shows a deeper chemocline
249 (Figure 3).

250 Specific conductance values were uniform down to 8 m in Josephine Lake during the
251 current study period (Figure 3). A chemocline was only detected below 11 m in May 2022, while
252 depths below 11 m were not assessed on other dates during the study period due to the difficulty
253 of finding the deepest area before mapping in 2022. Autumnal circulation down to 10 m was
254 reported in Josephine Lake in 1975 (Gage and Gorham 1985).

255



256
 257 Figure 3. Specific conductance profiles of a) Arco Lake, b) Budd Lake, c) Josephine Lake, and
 258 d) Deming Lake. For Deming Lake, seasons were classified according to solstice and equinox
 259 dates.



260

261 Figure 4. Hobo sensor data for temperature and conductance from Arco Lake, collected from
 262 May 2021 to May 2022 and from October 2021 to May 2022, respectively (top). Isotherm plot of
 263 the temperature data from the Hobo sensor (bottom).

264

265 Data from the temperature sensors (1.5, 3.5, 5.5, 7.5, 9.1, 9.5 m) and a conductance
 266 sensor (9.1 m) in Arco Lake from May 2021 to May 2022 are presented in Figure 4. In the
 267 summer of 2021, the temperature values in Arco Lake were different at distinct depths,
 268 representing the development of a summer thermocline. The temperatures at different depths
 269 started to converge in late fall until the lake became isothermal and continued cooling from 6 to
 270 4 C in mid-November 2021, representing the erosion of thermal stratification. The Brunt-Väisälä
 271 or buoyancy frequency (N), commonly expressed as N^2 in units s^{-2} , calculated from the time
 272 series temperature data is near zero at that time, indicating an erosion of stability, which
 273 persisted until the sensors were removed on May 16, 2022, over a week after the ice-off on May

274 8 (Supplementary Figure 4). A drop in the conductance value at 9.1 m in early November 2021
275 preceded isothermal conditions and indicated mixing down to at least 9.1 m (Figure 4). The
276 dimensionless lake number (Imberger and Patterson 1989) was calculated using the time series
277 and hourly wind data from Itasca State Park (Supplementary Figure 5). It started to consistently
278 rise on May 15, 2022 as the epilimnion warmed. In combination with the seasonally variable
279 chemocline depth (Figure 3), these analyses indicate that Arco Lake mixes during isothermal
280 periods and is not a meromictic lake. The data presented is most consistent with Arco being a
281 dimictic lake, although holomixis cannot be ruled out.

282 Data from the temperature sensors (0.5, 2.5, 5.5, 8.5, 11.5, and 14.5 m) in Deming Lake
283 from June 2019 to May 2020 are presented in Supplementary Figure 6. The lake became
284 isothermal in early November 2019. The Brunt-Väisälä frequency calculated from this data
285 dropped to near zero and rebounded slightly due to under-ice thermal stratification, a
286 phenomenon not observed in Arco Lake (Supplementary Figure 4). The specific conductance
287 profiles in Deming consistently show the same trend, although the exact depth and magnitude of
288 the chemocline vary seasonally and on the decadal scale (Figure 3). This indicates partial
289 seasonal mixing in Deming, likely during isothermal periods, but it may be insufficient or of too
290 short a duration to fully mix the lake. Deming was ice-free on April 25, 2020 (Minnesota
291 Department of Natural Resources 2022a), and the lake number started rising immediately due to
292 the onset of thermal stratification (Supplementary Figure 5), likely limiting the opportunity for
293 mixing. Long-term seasonal observation of a chemocline is consistent with Deming being a
294 meromictic lake (Zadereev et al. 2017).

295 Arco presents an end-member of a seasonally mixed lake (dimictic or holomictic) and
296 Deming an end-member of a meromictic lake among the four lakes studied here. In the absence

297 of high-frequency sensor profiles for Budd and Josephine lakes, the Schmidt stability
298 (Supplementary Figure 7) and the Brunt-Väisälä frequency (Supplementary Figures 8-11) were
299 calculated from seasonal profiles of temperature (Supplementary Figure 12) and salinity for all
300 four lakes. The Schmidt stability indicates that Deming and Budd are the most strongly stratified,
301 followed by Josephine and Arco. It is unknown when ice came off Budd Lake in 2022, but
302 Deming was ice-free on May 7, and Arco and Josephine were ice-free on May 8 (Minnesota
303 Department of Natural Resources 2022a) following strong winds on the evening of May 7.
304 Likely, Budd was also ice-free by May 8. A chemocline consistent with other summer
305 observations was present on May 17, 2022, which could indicate a lack of spring mixing for
306 Budd Lake. However, the January 2021 specific conductance profile for Budd shows a very
307 weak and deep chemocline, which would be expected from an autumn mixing event. Without
308 full profiles of specific conductance in Josephine Lake, it is impossible to evaluate mixing.
309 However, based on existing profiles, if a chemocline persists through spring turnover in
310 Josephine Lake as suggested by the sharp and deep chemocline observed in May 2022, then
311 monimolimnion must be limited to depths below 11 m, representing only 3.6% of total lake
312 volume (11,404.5 m³ of 313,295.5 m³).

313 Water color is related to the abundance of dissolved organic carbon (DOC) (Pace and
314 Cole 2002). Of the four study lakes, Budd had the most colored water, followed by Deming
315 (Supplementary Table 1). Arco and Josephine had very little color. Visually, Budd and Deming
316 appear brown, while Arco and Josephine appear green. Enhanced water color could lead to a
317 shallower thermocline and stronger stratification in Budd and Deming due to greater light
318 absorption by compounds conferring color (Houser 2006). The Brunt-Väisälä frequencies,
319 calculated from temperature and salinity profiles, are generally highest in the epilimnia during

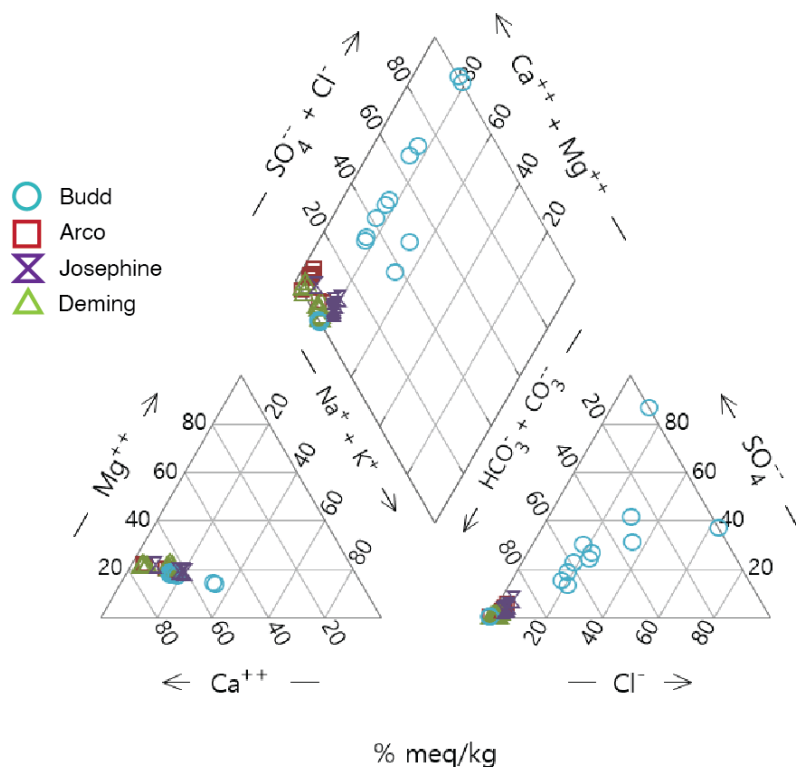
320 late summer (July 2021 and August 2022; Supplementary Figures 8-11). This indicates that
321 temperature is more important than salinity to the stability of these lakes. In August 2022, when
322 Deming Lake had the highest N^2 values observed, the meromictic stability (S') (Walker 1974)
323 was 7.81 J m^{-2} , within the range observed for the meromictic and ferruginous Lake 120 in
324 Canada (Campbell 1977) and Lake Nordbytjernet in Norway (Hongve 1999). These observations
325 suggest that meromixis in Deming Lake is primarily due to thermal stratification, with a small
326 contribution from salinity that could lead to meromixis in this lake but not the others nearby.
327 This phenomenon could be common to dilute meromictic lakes. In fact, a mixing event was
328 recorded for Deming Lake, in the summer of 1997, when a beaver dam west of the lake broke
329 and flooded it (Frane and Walberg 1997), indicating mixing can occur due to catastrophic events.

330

331

332

333



334

335 Figure 5. Piper Diagram of major cations and anions collected in May 2021.

336

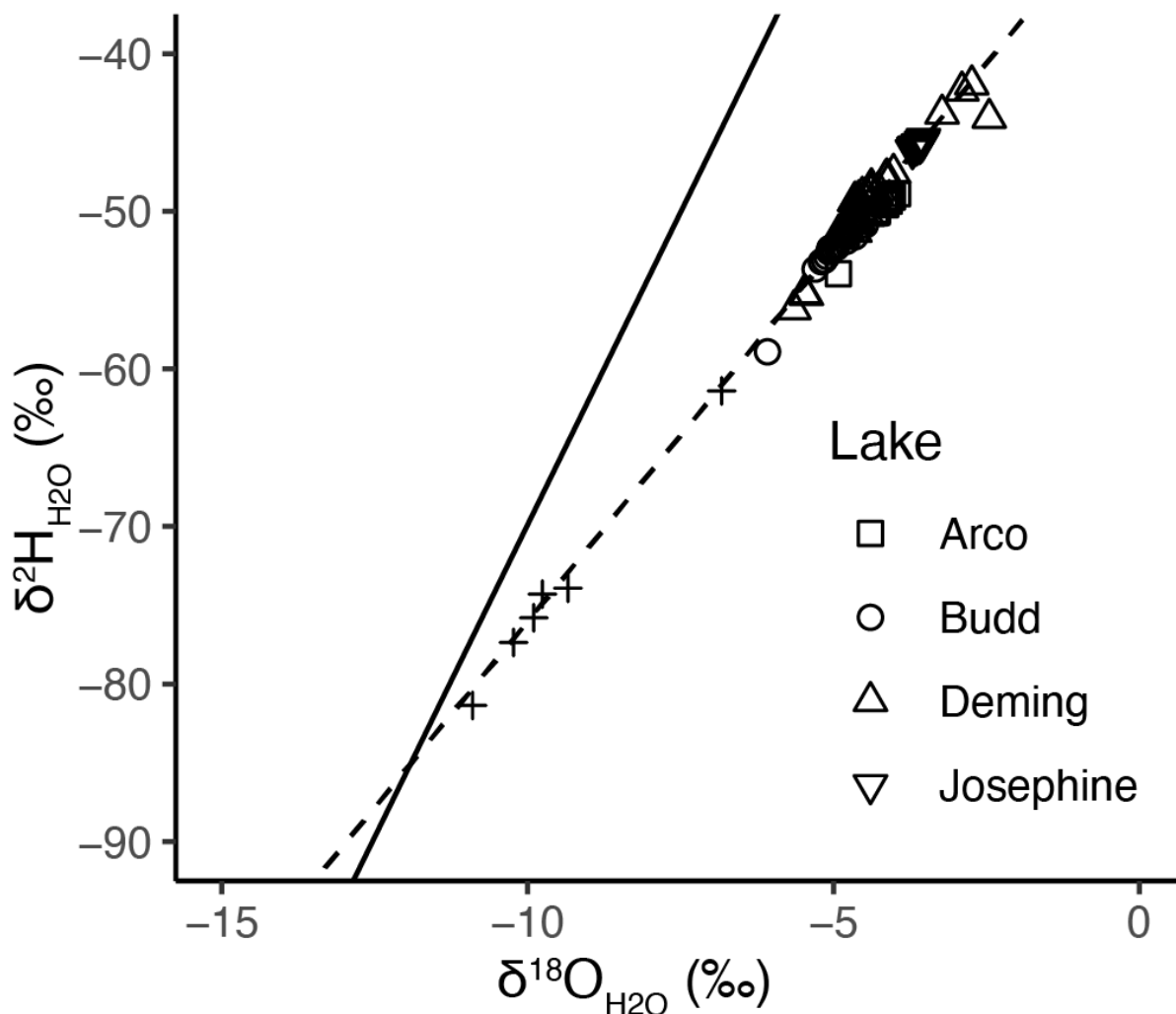
337 *Chemical Characteristics and Water Sources*

338 A Piper diagram was used to define the water types of the four lakes based on their major
 339 cations and anions. The predominant cation in all four study lakes was calcium (Figure 5). Budd
 340 had a greater proportion of milliequivalents from sodium and potassium than the other three
 341 lakes, balanced mostly by magnesium. Bicarbonate and carbonate ions represent nearly all anion
 342 milliequivalents in Deming, Arco, and Josephine whereas chloride and sulfate contribute to the
 343 anion balance in Budd. The water type for Deming, Arco, and Josephine is a calcium-
 344 bicarbonate type, whereas Budd does not have a dominant water type. The low specific
 345 conductance and lack of water type in Budd indicate the water source is predominantly

346 precipitation. Calcium, magnesium, and carbonate/bicarbonate ions source from the calcareous
347 Itasca moraine and are typical for the Itasca region (Megard et al. 1993). This indicates that
348 water supplying Deming, Arco, and Josephine has undergone more water-rock reaction than that
349 supplying Budd, such as might be expected from an increasing proportion of groundwater
350 seepage to a lake's water inputs. Deming, Arco, and Josephine lie in a tunnel valley channel
351 containing coarser sands and gravel while Budd Lake is poorly integrated hydrologically with
352 the other three lakes, and the net seepage in Budd is probably the lowest among all the lakes.
353 Arco (465.8 MAMSL) is located 51 meters north of Josephine (465.4 MAMSL) and Deming
354 (464.8 MAMSL) is located 284 meters north of Arco. The similar lake levels and wetlands
355 between Arco and Deming (Figures 1 and Supplementary Figure 1) indicate these lakes are
356 likely to be hydrologically connected. If the water table mimics the surface topography,
357 groundwater potentially flows from Arco-Josephine to Deming. However, Budd (478.6
358 MAMSL) is perched highest in the watershed, located off-axis of Deming-Arco-Josephine, to the
359 west of a ridge (Figure 1). Because it is perched, the ridge is likely composed of less permeable
360 material than the valley sediments, such as till. The presence of wetlands on the north end of
361 Budd that follow a small valley towards Deming suggests that there could be a surface or near
362 surface hydrological connection from Budd to Deming. Lakes highest in their watershed are
363 more likely to receive a greater proportion of water from precipitation (Kratz et al. 1997),
364 consistent with the dilute nature of Budd Lake.

365

366



367
 368 Figure 6. Isotope data and fit (dashed line) of an evaporation line ($\delta^2\text{H}_{\text{H}_2\text{O}} = 4.5 \cdot \delta^{18}\text{O}_{\text{H}_2\text{O}} - 29.9$,
 369 $r\text{-squared} = 0.93$) from the four study lakes plotted with a Local Meteoric Water Line (Stelling et
 370 al., 2021 Marcell Exp Forest). Crosses are spring or bog water data from Itasca State Park
 371 (Supplementary Table 1). The cross closest to the lake data points is the Deming bog. Analytical
 372 precision is within the symbol sizes.

373
 374 The isotopic composition of water (i.e., $\delta^2\text{H}_{\text{H}_2\text{O}}$ and $\delta^{18}\text{O}_{\text{H}_2\text{O}}$ in ‰) in May 2021 varied
 375 little with depth in each lake (Supplementary Figure 13). In Arco, Budd, and Deming sampled in

376 June 2019, the epilimnion waters become depleted relative to the deeper water. Additional
377 measurements at Deming Lake in July and October 2021 show enriched values in the epilimnion
378 relative to the surface. Preferential evaporation of light isotopes during the summer and early fall
379 drive the epilimnion to more enriched values. In Figure 6, all lakes data points diverge from a
380 local meteoric water line (LMWL; Stelling et al. 2021) on a lake evaporation line (LEL) with
381 equation $\delta^2\text{H}_{\text{H}_2\text{O}} (\text{‰}) = 4.5 * \delta^{18}\text{O}_{\text{H}_2\text{O}} (\text{‰}) - 29.9$. The intersection of the LMWL and the LEL is
382 the composition of regional groundwater, representing isotopically depleted snowmelt as the
383 predominant pathway for recharging the local aquifers (Krabbenhoft et al. 1994).

384 Historical $\delta^2\text{H}_{\text{H}_2\text{O}}$ and $\delta^{18}\text{O}_{\text{H}_2\text{O}}$ data from springs at Elk Lake were retrieved from the
385 Minnesota Spring Inventory (Minnesota Department of Natural Resources 2022b). The Elk Lake
386 springs were sampled again in May 2022, as well as a sample from Nicollet Creek and the bog
387 on the southeast side of Deming (Supplementary Table 1). These sites had abundant marsh
388 marigolds (Supplementary Figure 14), which bloom in May at groundwater discharge sites
389 (Rosenberry et al. 2000). The sites at Elk Lake and Nicollet Creek had visible iron
390 mineralization, indicating reducing, iron-bearing water discharge at the surface (Supplementary
391 Figure 14). The Nicollet Creek spring sample lies closest to the intersection of the LEL and
392 LMWL, whereas the Deming bog sample lies closest to the lakes but is more enriched than the
393 lakes (Figure 6).

394 The seasonal amplitude of a lake's isotopes can be used to calculate a lake's water
395 residence time (Engel and Magner 2019). A time series of temperature data from weather station
396 ITCM5 was used to determine average daily temperatures, and seasonal maximum and minimum
397 values were used to calculate the amplitude in $\delta^{18}\text{O}_{\text{H}_2\text{O}}$ inputs of precipitation. The Deming Lake
398 $\delta^{18}\text{O}_{\text{H}_2\text{O}}$ values (Supplementary Figure 13) encompass early spring, mid-summer, and late

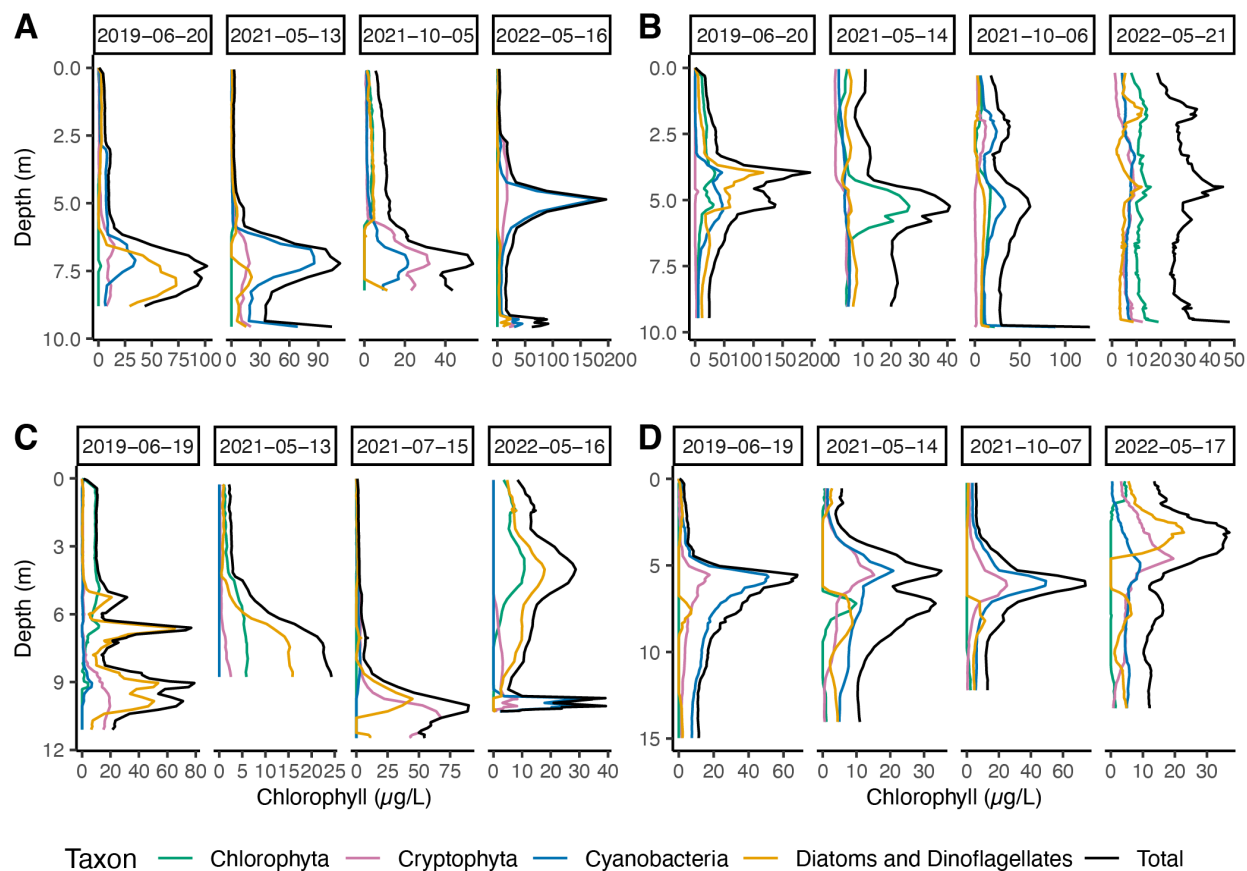
399 summer data, and were used to determine the seasonal amplitude in $\delta^{18}\text{O}_{\text{H}_2\text{O}}$ (Supplementary
400 Figure 15). These two values were used to estimate a mean water residence time of 100 days for
401 Deming Lake.

402

403 *Biological Characteristics*

404 Prior work on these four lakes indicated the presence of a lake-wide turbidity maximum
405 layer that was persistently just below 5 m Deming Lake (Baker and Brook 1971). This peak was
406 observable between late May and August from 1968-1970 but was absent in the winter. It was
407 reported in that study that bacteria and phytoplankton both contributed to the turbidity maximum
408 based on microscopic observations. This work indicated the layer was populated by the
409 cyanobacteria *Oscillatoria agardhii* var. *isothrix* (this genus is now called *Planktothrix*).

410

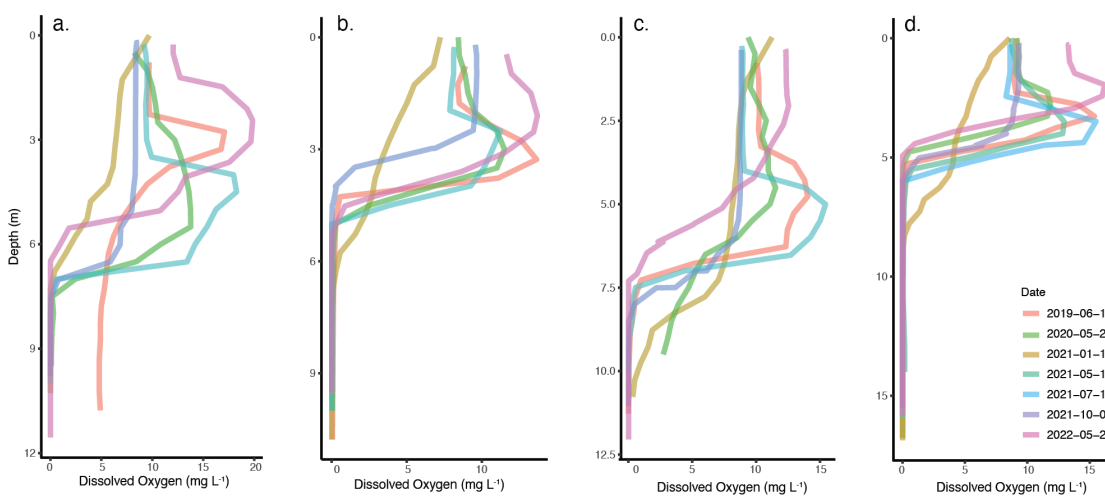


412 Figure 6. Multi-wavelength chlorophyll fluorescence (i.e. Fluoroprobe) measurements at a) Arco,
 413 b) Budd, c) Josephine, and d) Deming Lakes, showing seasonal and depth trends in major
 414 taxonomic groups. Note that the x scales vary between plots.

415
 416 From 2019 to 2022, chlorophyll-a measured via multi-wavelength fluorescence acquired
 417 with a Fluoroprobe allowed for deconvolution of the fluorescence signal so chlorophyll-a could
 418 be attributed to one of four taxonomic groups: Cyanobacteria, Chlorophyta, Diatoms and
 419 Dinophyta, or Cryptophyta. Taxon-specific concentrations of chlorophyll-a in each lake inform
 420 phytoplankton community structures with depth (Figure 6). Deming Lake has a persistent SCML
 421 around 5-6 m attributable to Cyanobacteria. The SCML is less distinct in May 2022, a week and
 422 a half after ice off. It was also less distinct in May 2021. This suggests that the SCML in Deming

423 Lake is a summer phenomenon that develops at or below the thermocline (Supplementary Figure
 424 12), consistent with the observations from Baker and Brook (1971). In June 2019, a profile of
 425 photosynthetically active radiation was also recorded (Supplementary Figure 19), and showed an
 426 inflection point at 5.5 m, corresponding to the depth of the SCML at that time. These
 427 observations are consistent with cyanobacteria forming a dense accumulation at that depth,
 428 attenuating the light flux into deeper waters.

429 Samples from the SCML were taken from the four lakes in May 2022: Arco (5 m), Budd
 430 (4.5 m), Deming (3.5 m), and Josephine (4.5 m). The most common phytoplankton of the four
 431 lakes were the cyanobacteria *Planktothrix* sp. and *Aphanocapsa* sp., and the green alga
 432 *Monoraphidium* sp. (Supplementary Figure 17). Some other phytoplankton species identified
 433 were the red alga *Cryptomonas* sp., the cyanobacteria *Planktolyngbya* sp. and *Dolichospermum*
 434 sp., as well as other colonial green algae and cyanobacteria species.



435
 436 Figure 7. Dissolved oxygen measurements at a) Arco, b) Budd, c) Josephine, and d) Deming
 437 Lakes, showing seasonal and depth trends.
 438

439 All four lakes have subsurface oxygen maxima exceeding air saturation during the
440 summer but lack this feature in the fall (Figure 7). The subsurface oxygen maximum in Deming
441 Lake usually occurs at 4 m, near the top of the thermocline (Church et al. 1989; Supplementary
442 Figure 12; Bieter et al. 1991; Balk et al. 2007). Metalimnetic oxygen maxima can result because
443 dissolved oxygen is more soluble in cold water after spring mixing, but as the water warms the
444 gas solubility decreases, causing oxygen to become supersaturated. Stratification induced by the
445 thermocline then limits the discharge of supersaturated oxygen to the atmosphere (Wilkinson et
446 al. 2015). Deming Lake rapidly develops a thermocline after ice-off (Supplementary Figure 6),
447 providing a mechanism for gas trapping. Enhanced biological productivity can also contribute to
448 the oxygen maximum, but is generally a smaller contributor (Craig et al. 1992; Wilkinson et al.
449 2015). The subsurface oxygen maximum is above the SCML in Deming Lake, suggesting that
450 the entrainment of spring oxygen is a larger contributor than photoautotrophy to the oxygen
451 maximum. However, there is also a pH maximum at that depth during the summer
452 (Supplementary Figure 18; Church et al. 1989; Barkow and Habedank 1990; Bieter et al. 1991),
453 as is expected for active photoautotrophy. Itasca Biological Station and Laboratories student
454 experiments that quantified photosynthesis and respiration via dissolved oxygen measurements
455 in bottle experiments generally found that net oxygen release was minimal in the SCML due to
456 vigorous respiration (Engstrom et al. 1974; Barkow and Habedank 1990). Measurements of the
457 O₂/Ar ratio would help to quantify the contribution of the two processes to the subsurface
458 oxygen maximum (Craig et al. 1992).

459 The occurrence of a summer SCML in Arco, Budd, and Josephine Lakes was more
460 variable than in Deming Lake (Figure 6). Arco had a spring bloom of cyanobacteria in May 2021
461 and in May 2022, at which time the highest chlorophyll-a of this study was recorded. At both

462 times, the SCML occurred below the oxygen maximum, in a hypoxic zone of the water column.
463 The May 2022 SCML at 5 m in Arco also enhanced light attenuation below that depth
464 (Supplementary Figure 19), as was observed in Deming in June 2019.

465 Arco, Budd, and Josephine also have subsurface oxygen maxima during summer,
466 although not as consistently as Deming. When the depth of the thermocline is plotted against the
467 depth of the oxygen maximum for all four lakes, there is a significant correlation if October 2021
468 samples are excluded (Supplementary Figure 20). In the fall, the subsurface oxygen maximum is
469 absent (highest values are at the surface), and the thermocline is deepest (Figure 7). This may
470 reflect that in fall the thermocline has deepened into hypoxic or anoxic waters.

471 **Conclusion**

472 Although reported to be meromictic, based on seasonal temperature and specific
473 conductance profiles, Arco, Budd and Josephine may be holomictic or even dimictic. Deming
474 has been meromictic in the periods of data collection presented here (2006-2009 and 2019-2022)
475 but experienced a mixing event in 1997 when an adjacent beaver dam broke. Although a
476 seasonally persistent chemocline occurs in Deming Lake, stratification is predominantly a
477 thermal phenomenon, with stability mostly conferred by a thermocline that develops rapidly after
478 isothermal spring and fall periods. Thermal stratification is not typical of meromictic lakes in the
479 temperate zone, but this weak stratification may be common in dilute boreal lakes (Meriläinen
480 1970; Campbell 1977). However, such meromixis may be easily perturbed by hydrographic or
481 land-use changes (Hongve 2002).

482 The chemical composition of the study lakes reflects their position in the watershed and
483 water sources. The highest-elevation lake, Budd, had no distinguishable water chemical type
484 and likely received most of its water from precipitation. Deming Lake had the highest ionic

485 load, consistent with a greater contribution of water that had undergone some water-rock
486 interaction, likely groundwater. Further work is necessary to characterize groundwater
487 composition and quantify and localize groundwater input to determine if Deming Lake could be
488 classified as crenogenic meromictic. The short water residence time in Deming Lake implied by
489 the analysis of $\delta^2\text{H}_{\text{H}_2\text{O}}$ and $\delta^{18}\text{O}_{\text{H}_2\text{O}}$, along with the minimal surface water inputs and likely high
490 permeability of tunnel valley deposits suggest the shallow groundwater system should be
491 considered as a major water source.

492 All four lakes have SCML during summer. The depth of the SCML varies in Arco, Budd,
493 and Josephine and is sometimes absent, but persists at around 5 m in Deming, corresponding to
494 the base of the photic zone. Subsurface oxygen maxima above air saturation likely develop by
495 trapping gas in cold water that then warms with rapid thermocline development in the spring.
496 Corresponding pH maxima in Arco and Deming indicate that primary productivity could also
497 contribute to the subsurface oxygen maxima.

498 **Acknowledgments**

499 This work was supported by a National Science Foundation CAREER award to EDS (1944946).
500 The GeoAllies program, funded by the National Science Foundation, supported student
501 participation in the GEOL 406/506 field course, as well as funds from the Department of
502 Geological & Atmospheric Sciences at Iowa State University. Support for the field course was
503 also provided by Dr. Jonathan Schilling, Director of the Itasca Biological Station and
504 Laboratories, and Dr. Emily Schilling. Phytoplankton was identified at the genus level with the
505 help of Dr. Lesley Knoll, Associate Director of the Itasca Biological Station and Laboratories,
506 who also provided assistance with field operations for the duration of the 2019-2022 field
507 seasons. Chad Wittkop and Moses Lado (Minnesota State University) assisted with fieldwork in

508 2019. Jazlyn Beeck and Elise Bauer (Iowa State University) assisted with fieldwork in 2021.
509 Julia Kelly and Shannon Farrell of the University of Minnesota Library assisted with accessing
510 Itasca Biological Station and Laboratories student reports.

511

512 **References**

513 Anderson, R. Y., and W. E. Dean. 1988. Lacustrine varve formation through time. *Palaeogeogr.*
514 *Palaeoclimatol. Palaeoecol.* **62**: 215–235. doi:10.1016/0031-0182(88)90055-7

515 Anderson, R. Y., W. E. Dean, P. Bradbury, and D. Love. 1985. *Meromictic Lakes and Varved*
516 *Lake Sediments in North America.*

517 Baker, A., and A. Brook. 1971. Optical density profiles as an aid to the study of microstratified
518 phytoplankton populations in lakes. *Arch. für Hydrobiol.* **69**: 214–233.

519 Balk, D., A. Graetz, A. Morantes, and D. Olson. 2007. Itasca Biological Station Student Report
520 2485: Comparative investigation of zooplankton diel vertical migration patterns in Arco and
521 Deming Lake: the effect of predation. University of Minnesota.

522 Barkow, M., and T. Habedank. 1990. Itasca Biological Station Student Report 1906: A
523 Limnological study of Demming Lake.

524 Barnes, P., T. Halpern, and T. Meier. 1976. Itasca Biological Station Student Report 1157: A
525 limnological investigation of Arco Lake. University of Minnesota.

526 Bieter, J., G. Romig, and J. Waugh. 1991. Itasca Biological Station Student Report 1905: An
527 ecological study of the meromictic Deming Lake. University of Minnesota.

528 Boehrer, B., and M. Schultze. 2008. Stratification of lakes. *Rev. Geophys.* **46**.
529 doi:10.1029/2006RG000210

530 Callis, J., M. R. Hummon, and P. Skerrett. 1976. Itasca Biological Station Student Report 1158:

- 531 Lake Josephine, Summer 1976. University of Minnesota.
- 532 Camacho, A. 2006. On the occurrence and ecological features of deep chlorophyll maxima
533 (DCM) in Spanish stratified lakes. *Limnetica* **25**: 453–478.
- 534 Campbell, P. 1977. Descriptive limnology of Lake 120, a meromictic lake on the Precambrian
535 Shield in northwestern Ontario. University of Manitoba.
- 536 Church, T., M. Tillotson, and L. Wendler. 1989. Itasca Biological Station Student Report 1830:
537 Survey of the meromictic Demming Lake, Summer 1989. University of Minnesota.
- 538 Condon, M., K. A. Sokol, and D. J. Wilson. 1996. Itasca Biological Station Student Report
539 2134:Deming Lake, MN: a limnological inquiry. University of Minnesota.
- 540 Craig, A. H., R. A. Wharton, C. P. McKay, S. Science, N. Series, and N. Jan. 1992. Oxygen
541 Supersaturation in Ice-Covered Antarctic Lakes : Biological Versus Physical Contributions.
542 *Science* (80-.). **255**: 318–321.
- 543 Cuthbert, I. D., and P. del Giorgio. 1992. Toward a standard method of measuring color in
544 freshwater. *Limnol. Oceanogr.* **37**: 1319–1326. doi:10.4319/lo.1992.37.6.1319
- 545 Dean, W. E., and A. Schwalb. 2002. The lacustrine carbon cycle as illuminated by the waters and
546 sediments of two hydrologically distinct headwater lakes in North-Central Minnesota,
547 U.S.A. *J. Sediment. Res.* **72**: 416–431. doi:10.1306/101801720416
- 548 Degens, E. T., and P. Stoffers. 1976. Stratified waters as a key to the past. *Nature* **263**: 22–27.
549 doi:10.1038/263022a0
- 550 Engel, L., and J. Magner. 2019. Estimating the direction of lake hydraulic residence in
551 Minnesota’s sentinel lakes: implications for management. *Int. J. Hydrol.* **3**: 362–367.
552 doi:10.15406/ijh.2019.03.00201
- 553 Engstrom, G., B. Dahl, D. Nelson, and D. Netko. 1974. Itasca Biological Station Student Report

- 554 777: An ecological study of Deming Lake. University of Minnesota.
- 555 Evans, J., and D. Bjerklie. 1975. Itasca Biological Station Student Report 842: Some
556 limnological investigations of Arco Lake, Itasca State Park, Minnesota. University of
557 Minnesota.
- 558 Frane, M. A., and T. J. Walberg. 1997. Itasca Biological Station Student Report 2260: Arco and
559 Demming: Two Worlds Divided, Demming: When the Levee Breaks.
- 560 Gage, M. A., and E. Gorham. 1985. Alkaline phosphatase activity and cellular phosphorus as an
561 index of the phosphorus status of phytoplankton in Minnesota lakes. *Freshw. Biol.* **15**: 227–
562 233. doi:10.1111/j.1365-2427.1985.tb00195.x
- 563 Habedank, T. 1990. Itasca Biological Station Student Report 2211: Chlorophyll analysis and
564 general physical and chemical profile of Demming Lake. University of Minnesota.
- 565 Hakala, A. 2004. Meromixis as a part of lake evolution - observations and a revised classification
566 of true meromictic lakes in Finland. *Boreal Environ. Res.* **9**: 37–53.
- 567 Hall, K., and T. Northcote. 2012. Meromictic Lakes, p. 519–524. *In* L. Bengtsson, R. Herschy,
568 and R. Fairbridge [eds.], *Encyclopedia of Lakes and Reservoirs*.
- 569 Harren, S., J. Kartak, J. Knight, and J. Lehman. 2011. The effects of fish presence and mixing
570 patterns on water clarity in lakes: Arco, Deming, and Itasca. University of Minnesota.
- 571 Hongve, D. 1999. Long-term Variation in the Stability of the Meromictic Lake Nordbytjernet
572 Caused by Groundwater Fluctuations. *Nord. Hydrol.* **30**: 21–38.
- 573 Hongve, D. 2002. Seasonal Mixing and Genesis of Endogenic Meromixis in Small Lakes in
574 Southeast Norway. *Hydrol. Res.* **33**: 189 LP – 206.
- 575 Hooper, F. F. 1951. Limnological Features of a Minnesota Seepage Lake. *Am. Midl. Nat.* **46**:
576 462–481. doi:10.2307/2421989

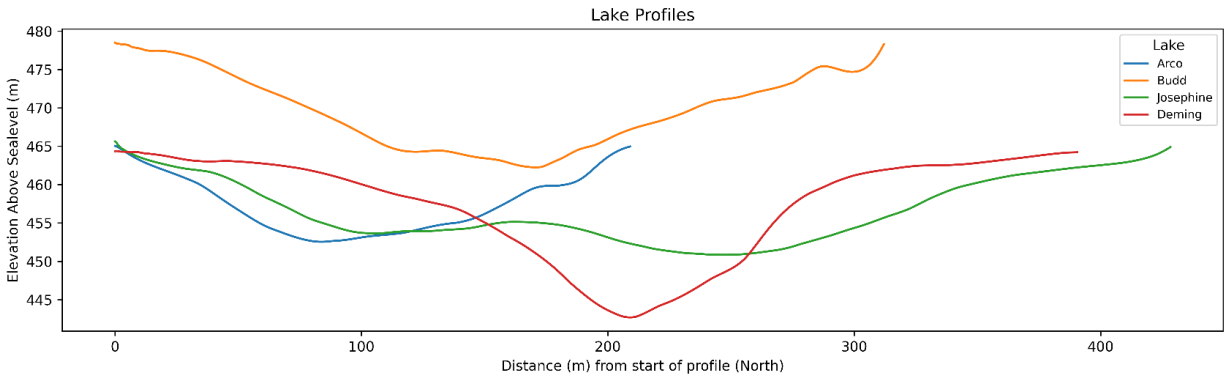
- 577 Houser, J. N. 2006. Water color affects the stratification, surface temperature, heat content, and
578 mean epilimnetic irradiance of small lakes. *Can. J. Fish. Aquat. Sci.* **63**: 2447–2455.
579 doi:10.1139/F06-131
- 580 Imberger, J., and J. C. Patterson. 1989. Physical Limnology, p. 303–475. *In* J.W. Hutchinson and
581 T.Y.B.T.-A. in A.M. Wu [eds.]. Elsevier.
- 582 Jellison, R., and J. M. Melack. 1993. Meromixis in hypersaline Mono Lake, California. 1.
583 Stratification and vertical mixing during the onset, persistence, and breakdown of
584 meromixis. *Limnol. Oceanogr.* **38**: 1008–1019. doi:10.4319/lo.1993.38.5.1008
- 585 Jennings, C. E., and M. D. Johnson. 2011. The Quaternary of Minnesota, *In* J. Ehlers, P.L.
586 Gibbard, and P.D. Hughes [eds.], *Quaternary Glaciations Extent and Chronology, Part IV -*
587 *a closer look.*
- 588 Karli, J., and C. Keller. 1975. Itasca Biological Station Student Report 803: A presentation of the
589 data collected on Deming Lake through the course of Aquatic Ecology. University of
590 Minnesota.
- 591 Katsev, S., S. A. Crowe, A. Mucci, B. Sundby, S. Nomosatryo, G. D. Haffner, and D. A. Fowle.
592 2010. Mixing and its effects on biogeochemistry in persistently stratified, deep, tropical
593 Lake Matano, Indonesia. *Limnol. Ocean.* **55**: 763–776.
- 594 Kjensmo, J. 1967. The development and some main features of “iron-meromictic” soft water
595 lakes. *Arch. Hydrobiol.* **32**: 137–312.
- 596 Klausmeier, C. A., and E. Litchman. 2001. Algal games: The vertical distribution of
597 phytoplankton in poorly mixed water columns. *Limnol. Oceanogr.* **46**: 1998–2007.
598 doi:10.4319/lo.2001.46.8.1998
- 599 Knoll, L. B., and J. B. Cotner. 2018. University of Minnesota Itasca Biological Station and

- 600 Laboratories: Over 100 Years of Field-based Education and Research. *Limnol. Oceanogr.*
601 *Bull.* **27**: 42–44.
- 602 Krabbenhoft, D. P., C. J. Bowser, C. Kendall, and J. R. Gat. 1994. Use of Oxygen-18 and
603 Deuterium To Assess the Hydrology of Groundwater-Lake Systems. 67–90.
604 doi:10.1021/ba-1994-0237.ch003
- 605 Kratz, T. K., K. E. Webster, C. J. Bowser, J. J. Magnuson, and B. J. Benson. 1997. The influence
606 of landscape position on lakes in northern Wisconsin. *Freshw. Biol.* **37**: 209–217.
607 doi:10.1046/j.1365-2427.1997.00149.x
- 608 Lascu, I., K. K. McLauchlan, A. Myrbo, P. R. Leavitt, and S. K. Banerjee. 2012. Sediment-
609 magnetic evidence for last millennium drought conditions at the prairie–forest ecotone of
610 northern United States. *Palaeogeogr. Palaeoclimatol. Palaeoecol.* **337–338**: 99–107.
611 doi:<https://doi.org/10.1016/j.palaeo.2012.04.001>
- 612 Lascu, I., and C. Plank. 2013. A new dimension to sediment magnetism: Charting the spatial
613 variability of magnetic properties across lake basins. *Glob. Planet. Change* **110**: 340–349.
614 doi:10.1016/j.gloplacha.2013.03.013
- 615 Ledesma, G. M., R. Islam, and E. D. Swanner. 2022. Evaluation of preservation protocols for
616 oxygen-sensitive minerals within laminated aquatic sediments. *EarthArXiv*.
617 doi:10.31223/X5M068
- 618 Ludlam, S. D., and B. Duval. 2001. Natural and management-induced reduction in
619 monimolimnetic volume and stability in a Coastal, Meromictic Lake. *Lake Reserv. Manag.*
620 **17**: 71–81. doi:10.1080/07438140109353975
- 621 McLauchlan, K. K., A. Myrbo, I. Lascu, and P. R. Leavitt. 2013. Variable ecosystem response to
622 climate change during the Holocene in northern Minnesota, USA. *GSA Bull.* **125**: 445–452.

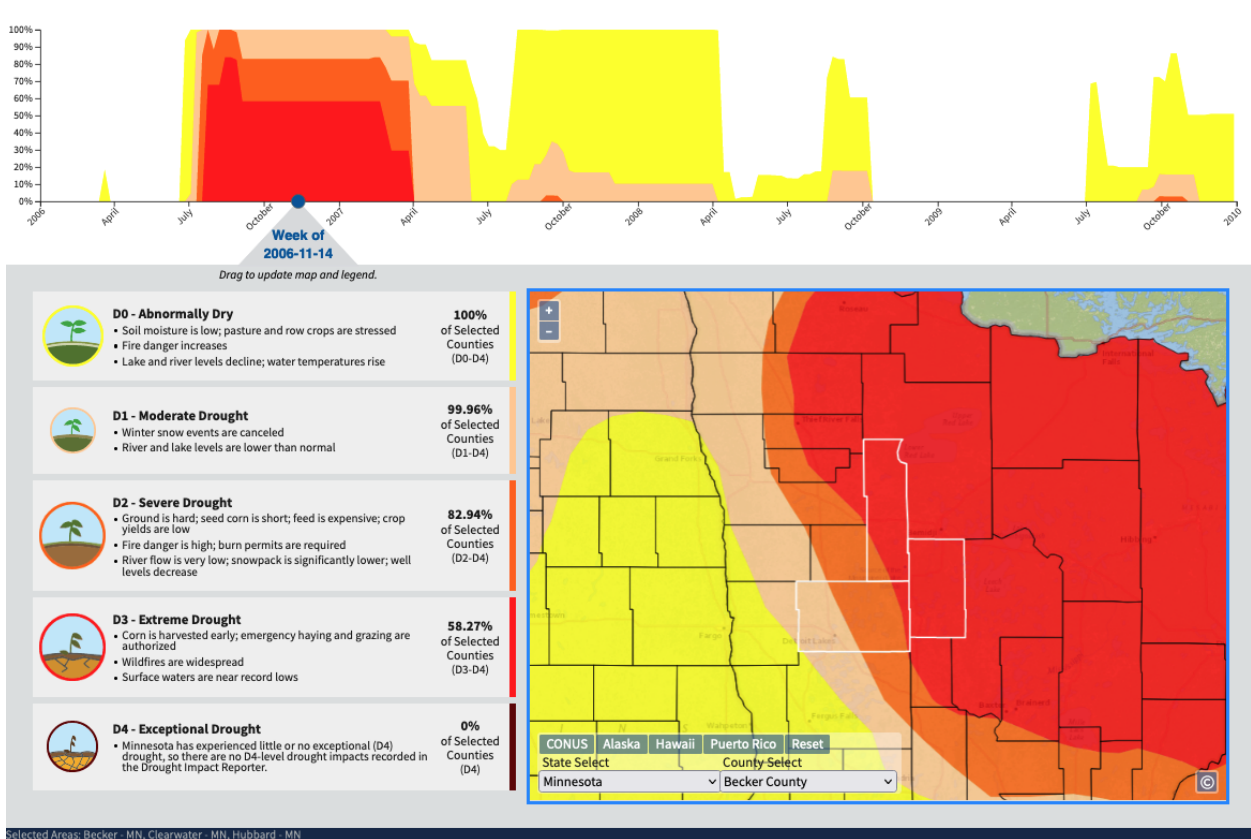
- 623 doi:10.1130/B30737.1
- 624 Megard, R. O., J. P. Bradbury, and W. E. Dean. 1993. Climatic and limnologic setting of Elk
625 Lake, *In* Bradbury, J. P. and W.E. Dean [eds.], Elk Lake, Minnesota: Evidence for Rapid
626 Climate Change in the North-Central United States. The Geological Society of America.
- 627 Meriläinen, J. 1970. On the limnology of the meromictic Lake Valkiajärvi, in the Finnish Lake
628 District. *Ann. Bot. Fenn.* **7**: 29–51.
- 629 Minnesota Department of Natural Resources. 2022a. Lake Ice Out Dates.
- 630 Minnesota Department of Natural Resources. 2022b. Minnesota Spring Inventory.
- 631 National Oceanographic and Atmospheric Administration. National Integrated Drought
632 Information System.
- 633 Nelson, R., J. Henry, M. Al-Shamisi, and T. Clifford. 2011. The effects of wind exposure on
634 microorganism stratification and distribution in Lake Itasca and Deming Lake. University of
635 Minnesota.
- 636 O’Sullivan, P. E. 1983. Annually-laminated lake sediments and the study of Quaternary
637 environmental changes — a review. *Quat. Sci. Rev.* **1**: 245–313.
638 doi:[https://doi.org/10.1016/0277-3791\(83\)90008-2](https://doi.org/10.1016/0277-3791(83)90008-2)
- 639 Pace, M. L., and J. J. Cole. 2002. Synchronous variation of dissolved organic carbon and color in
640 lakes. *Limnol. Oceanogr.* **47**: 333–342. doi:10.4319/lo.2002.47.2.0333
- 641 Pilati, A., and W. A. Wurtsbaugh. 2003. Importance of zooplankton for the persistence of a deep
642 chlorophyll layer: A limnocorral experiment. *Limnol. Oceanogr.* **48**: 249–260.
643 doi:10.4319/lo.2003.48.1.0249
- 644 Reiter, C., J. Schmitz, and S. Helfman. 1998. Itasca Biological Station Student Report 2318: A
645 limnological study of Deming Lake. University of Minnesota.

- 646 Rosenberry, D. O., R. G. Streigl, and D. C. Hudson. 2000. Plants as indicators of focused ground
647 water discharge to a northern Minnesota lake. *Ground Water*.
- 648 Schultze, M., B. Boehrer, K. Wendt-Potthoff, S. Katsev, and E. T. Brown. 2017. Chemical
649 Setting and Biogeochemical Reactions in Meromictic Lakes BT - Ecology of Meromictic
650 Lakes, p. 35–59. *In* R.D. Gulati, E.S. Zadereev, and A.G. Degermendzhi [eds.]. Springer
651 International Publishing.
- 652 Stelling, J. M., S. D. Sebestyen, N. A. Griffiths, C. P. J. Mitchell, and M. B. Green. 2021. The
653 stable isotopes of natural waters at the Marcell Experimental Forest. *Hydrol. Process.* **35**: 1–
654 9. doi:10.1002/hyp.14336
- 655 Stewart, K. M., K. F. Walker, and G. E. Likens. 2009. Meromictic Lakes, p. 589–602. *In*
656 G.E.B.T.-E. of I.W. Likens [ed.], *Encyclopedia of Inland Waters*. Academic Press.
- 657 Swanner, E. D., N. Lambrecht, C. Wittkop, C. Harding, S. Katsev, J. Torgeson, and S. W.
658 Poulton. 2020. The biogeochemistry of ferruginous lakes and past ferruginous oceans.
659 *Earth-Science Rev.* **211**: 103430. doi:10.1016/j.earscirev.2020.103430
- 660 Swanner, E. D., I. Lascu, C. Harding, G. M. Ledesma, T. Leung, and S. A. Akam. 2022. Water
661 properties of Arco Lake, Budd Lake, Deming Lake, and Josephine Lake in Itasca State Park
662 from 2006-2009 and 2019-2021, v. 2. *Environ. Data Initiat.*
663 doi:10.6073/pasta/692c92ef1c8291162732c2b98cebdaea
- 664 U.S. Geological Survey. 2017. Watershed Boundary Dataset.
- 665 Walker, K. F. 1974. The stability of meromictic lakes in central Washington. *Limnol. Oceanogr.*
666 **19**: 209–222. doi:10.4319/lo.1974.19.2.0209
- 667 Walker, K. F., and G. E. Likens. 1975. Meromixis and a reconsidered typology of lake
668 circulation patterns. *Verh Intern. Verein Limnol* **19**: 442–458.

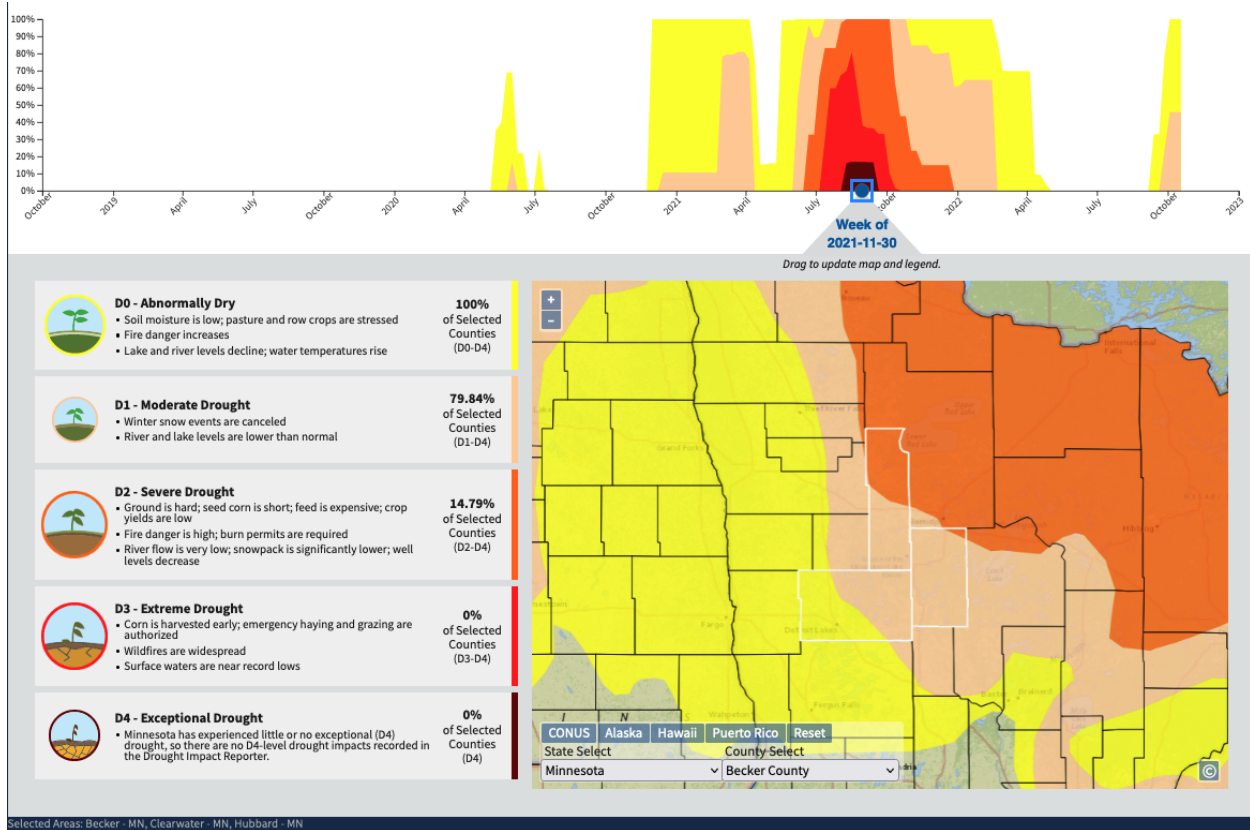
- 669 doi:10.1080/03680770.1974.11896084
- 670 Wetzel, R. G. 2001. *Limnology: Lake and River Ecosystems*, Third. Academic Press.
- 671 Wilkinson, G. M., J. J. Cole, M. L. Pace, R. A. Johnson, and M. J. Kleinmans. 2015. Physical and
672 biological contributions to metalimnetic oxygen maxima in lakes. *Limnol. Oceanogr.* **60**:
673 242–251. doi:10.1002/lno.10022
- 674 Winslow, L. A., J. S. Read, R. Woolway, J. A. Brentrup, T. H. Leach, J. A. Zwart, S. Albers, and
675 D. Collinge. 2019. rLakeAnalyzer.
- 676 Wittkop, C., E. D. Swanner, A. Grengs, and others. 2020. Evaluating a primary carbonate
677 pathway for manganese enrichments in reducing environments. *Earth Planet. Sci. Lett.* **538**:
678 116201. doi:<https://doi.org/10.1016/j.epsl.2020.116201>
- 679 Wittkop, C., J. Teranes, B. Lubenow, and W. E. Dean. 2014. Carbon- and oxygen-stable isotope
680 signatures of methanogenesis, temperature, and water column stratification in Holocene
681 siderite varves. *Chem. Geol.* **389**: 153–166. doi:10.1016/j.chemgeo.2014.09.016
- 682 Wright Jr., H. E. 1993. History of the landscape in the Itasca region, p. 7–17. *In* J.P. Bradbury
683 and W.E. Dean [eds.], *Elk Lake, Minnesota: Evidence for Rapid Climate Change in the*
684 *North-Central United States*. United States Geological Survey.
- 685 Zadereev, E. S., B. Boehrer, and R. D. Gulati. 2017. Introduction: Meromictic Lakes, Their
686 Terminology and Geographic Distribution, p. 1–11. *In* R.D. Gulati, E.S. Zadereev, and A.G.
687 Degermendzhi [eds.], *Ecology of Meromictic Lakes*. Springer International Publishing.
- 688
- 689



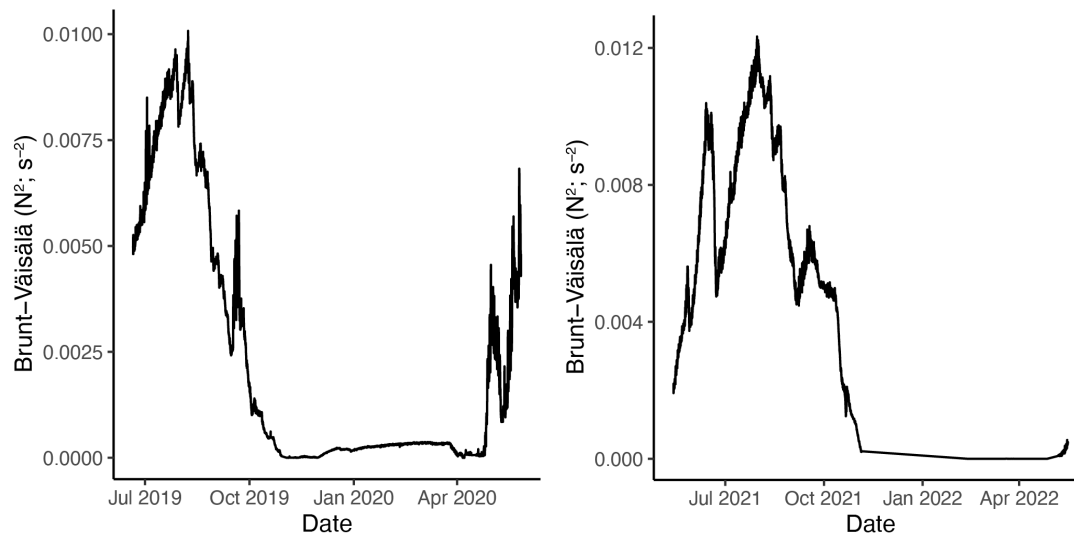
Supplementary Figure 1. Profiles of the lakes (in meters above mean sea level) along the fence diagrams in Figure 1.



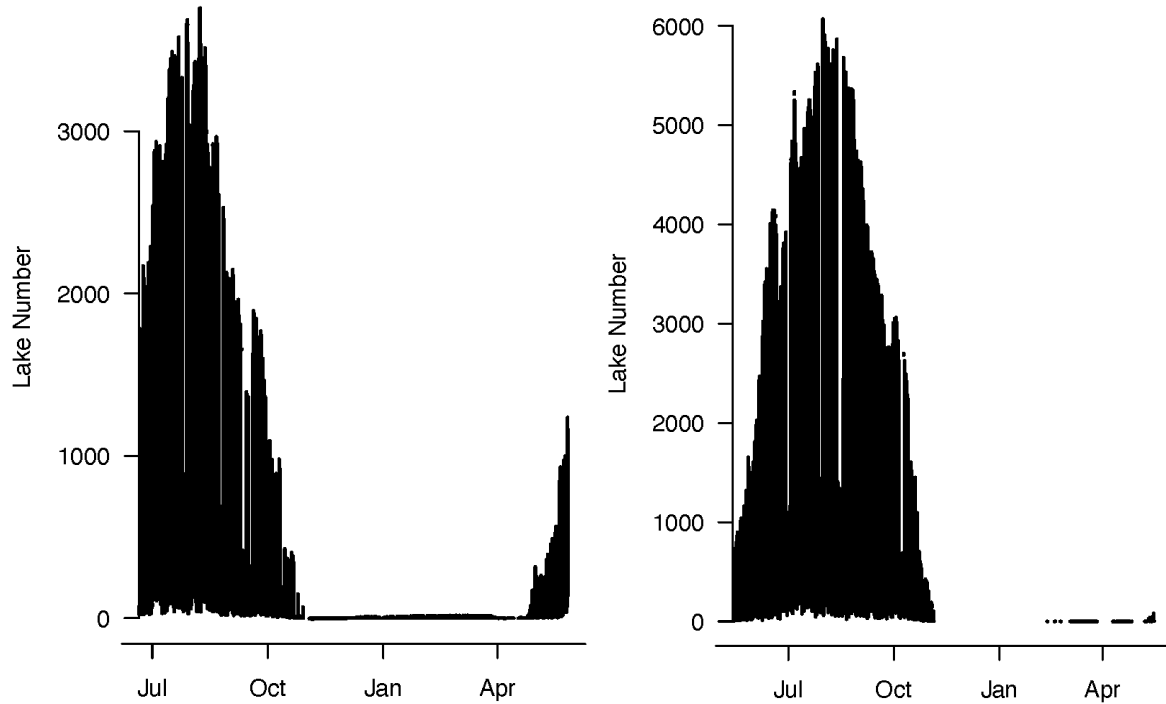
Supplementary Figure 2. Historical drought information for the counties encompassing Itasca State Park during the period of data collection from 2006-2009.



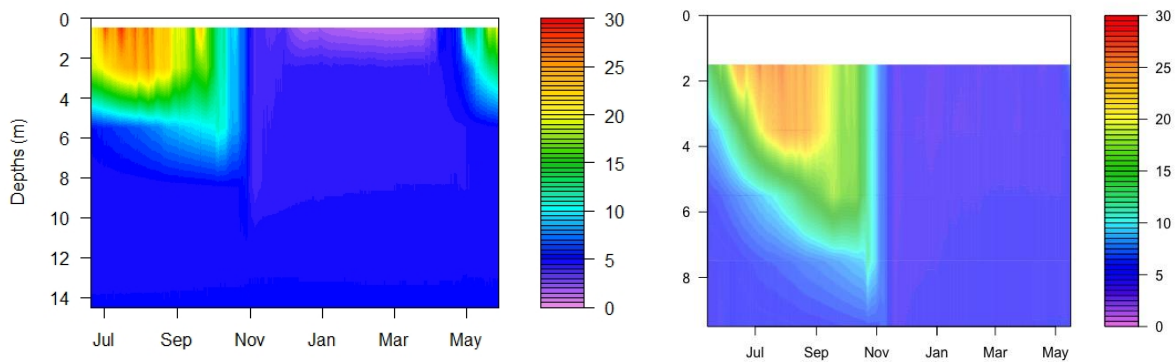
Supplementary Figure 3. Historical drought information for the counties encompassing Itasca State Park during the period of data collection from 2019-2022 (retrieved on October 24, 2022).



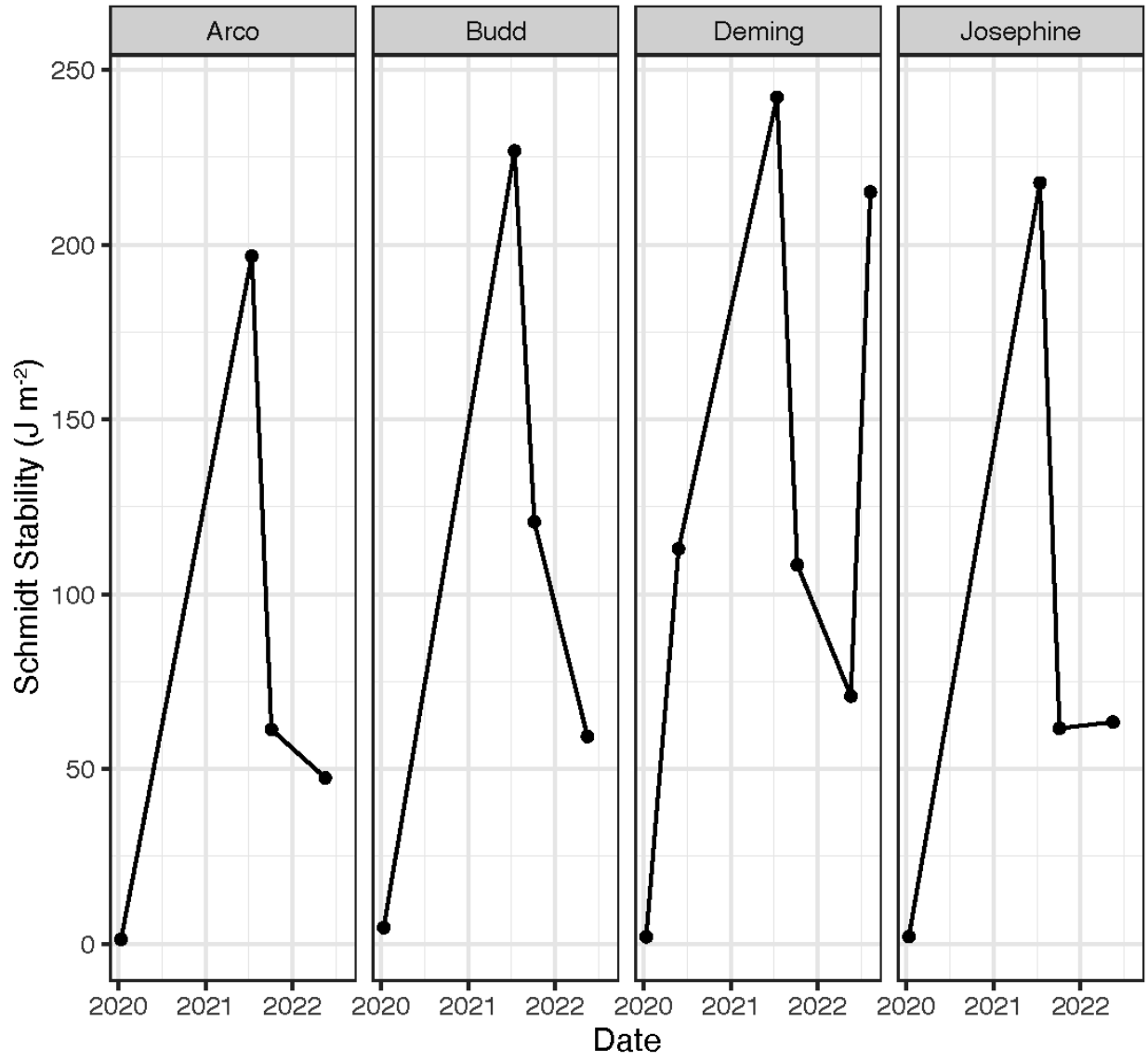
Supplementary Figure 4. The Brunt-Väisälä or buoyancy frequency (N^2 , s^{-2}), calculated from the temperature time series for Deming Lake from June 2019 to May 2020 (left), and Arco Lake from May 2021 to May 2022 (right). Higher values indicate greater stability.



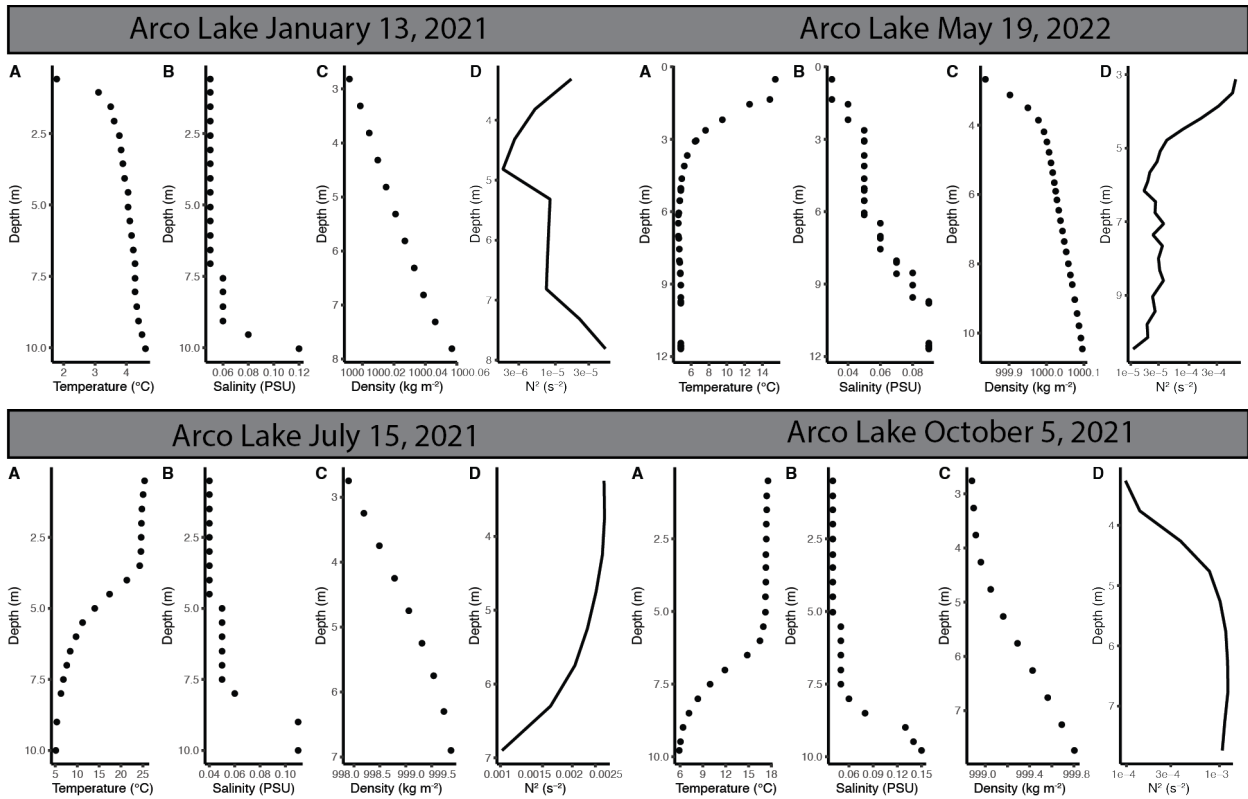
Supplementary Figure 5. The dimensionless lake number was calculated using wind speeds from the ITCM5 weather station and the temperature time series for Deming Lake from June 2019 to May 2020 (left), and Arco Lake from May 2021 to May 2022 (right). Higher values indicate greater stability.



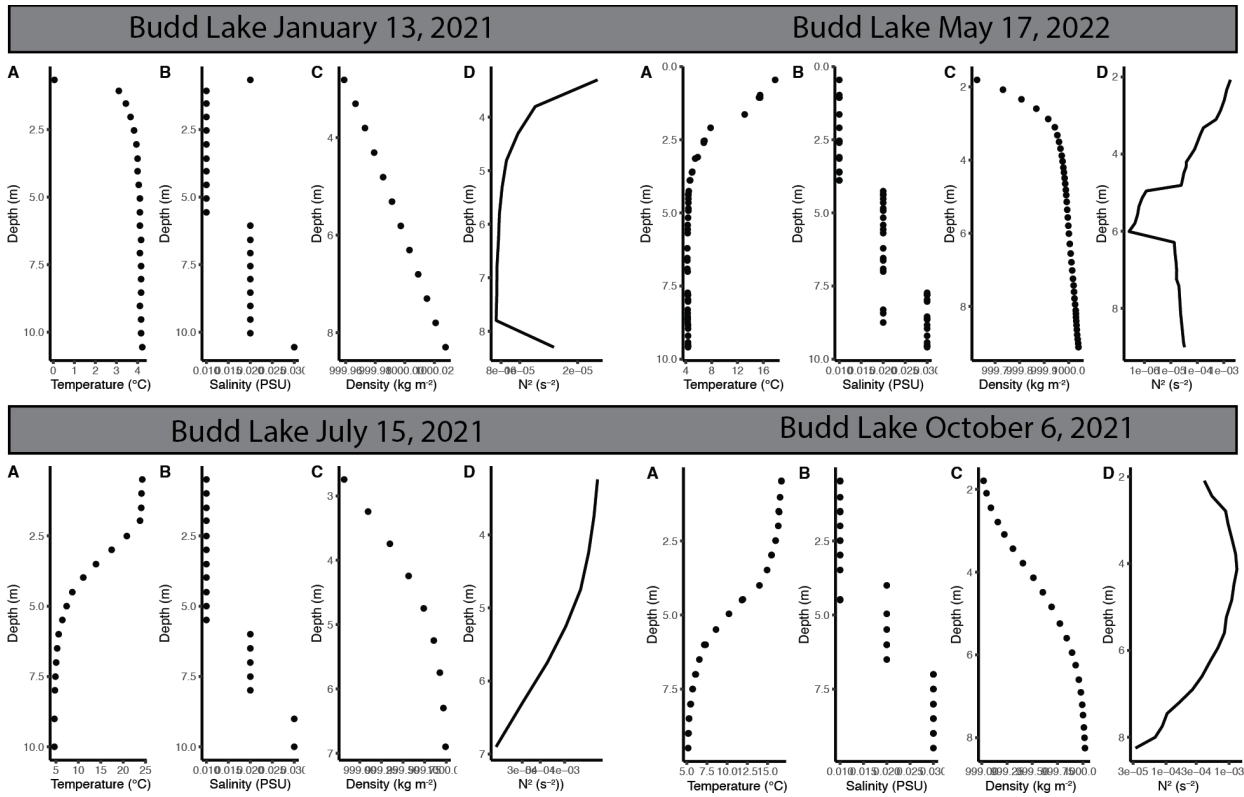
Supplementary Figure 6. Deming Lake temperatures (C) from June 2019 to May 2020 (left). Arco Lake temperatures (C) from May 2021 to May 2022 (right).



Supplementary Figure 7. Plots of Schmidt Stability for each of the four study lakes from January 2021 to August 2022. Higher values indicate greater stability.

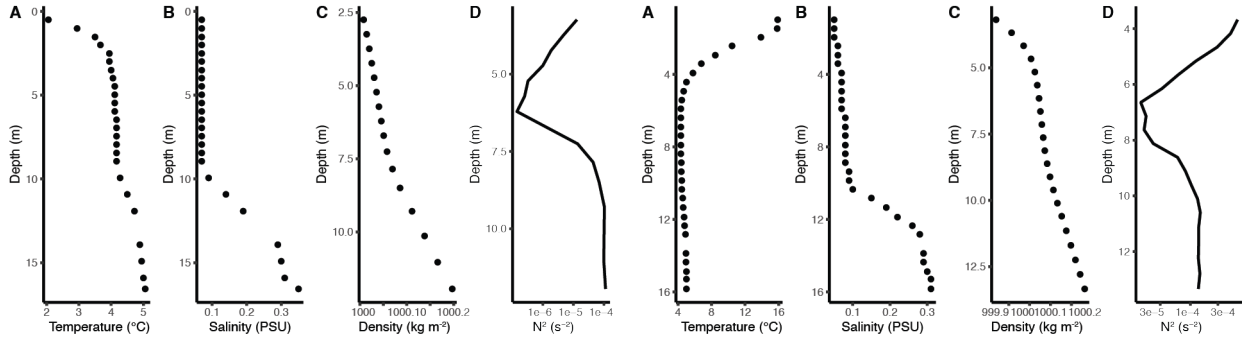


Supplementary Figure 8. The Brunt-Väisälä or buoyancy frequency (N^2 , s^{-2}), calculated from the temperature and salinity profiles from Arco Lake from January 2021 to May 2022. Higher values indicate greater stability.

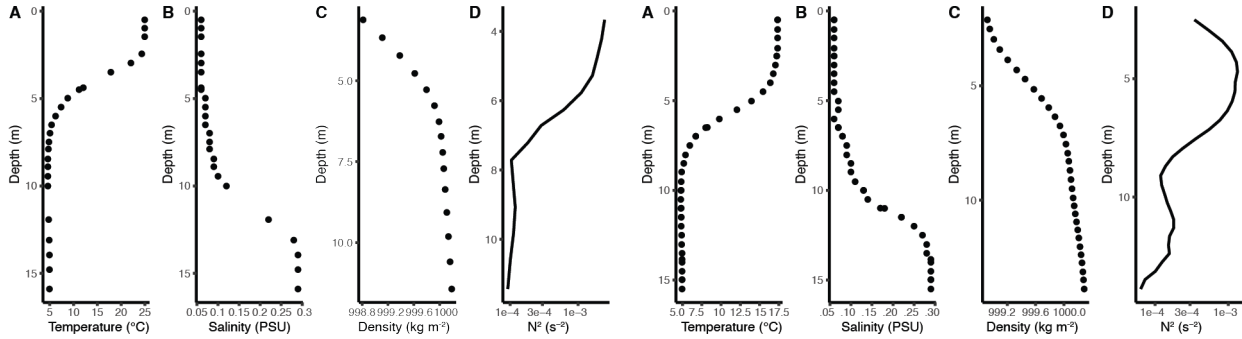


Supplementary Figure 9. The Brunt-Väisälä or buoyancy frequency (N^2 , s^{-2}), calculated from the temperature and salinity profiles from Budd Lake from January 2021 to May 2022. Higher values indicate greater stability.

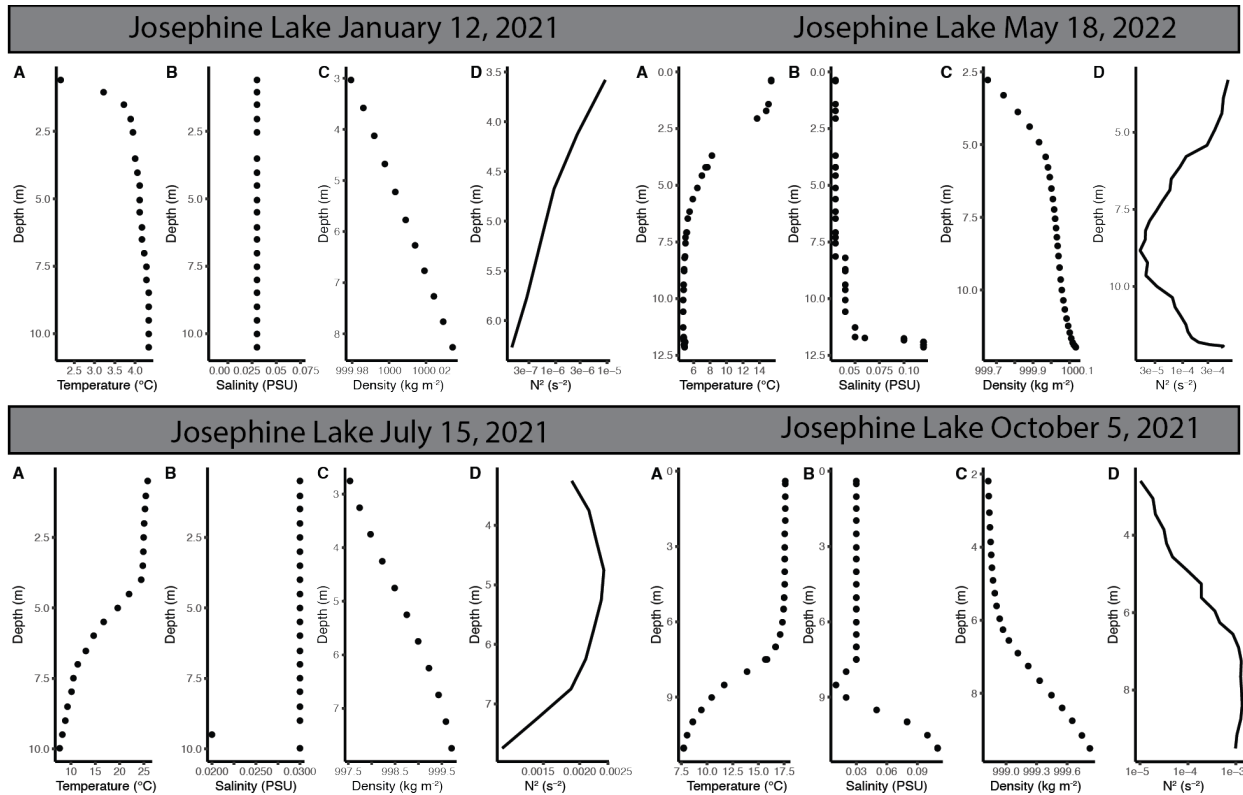
Deming Lake January 12, 2021 Deming Lake May 20, 2022



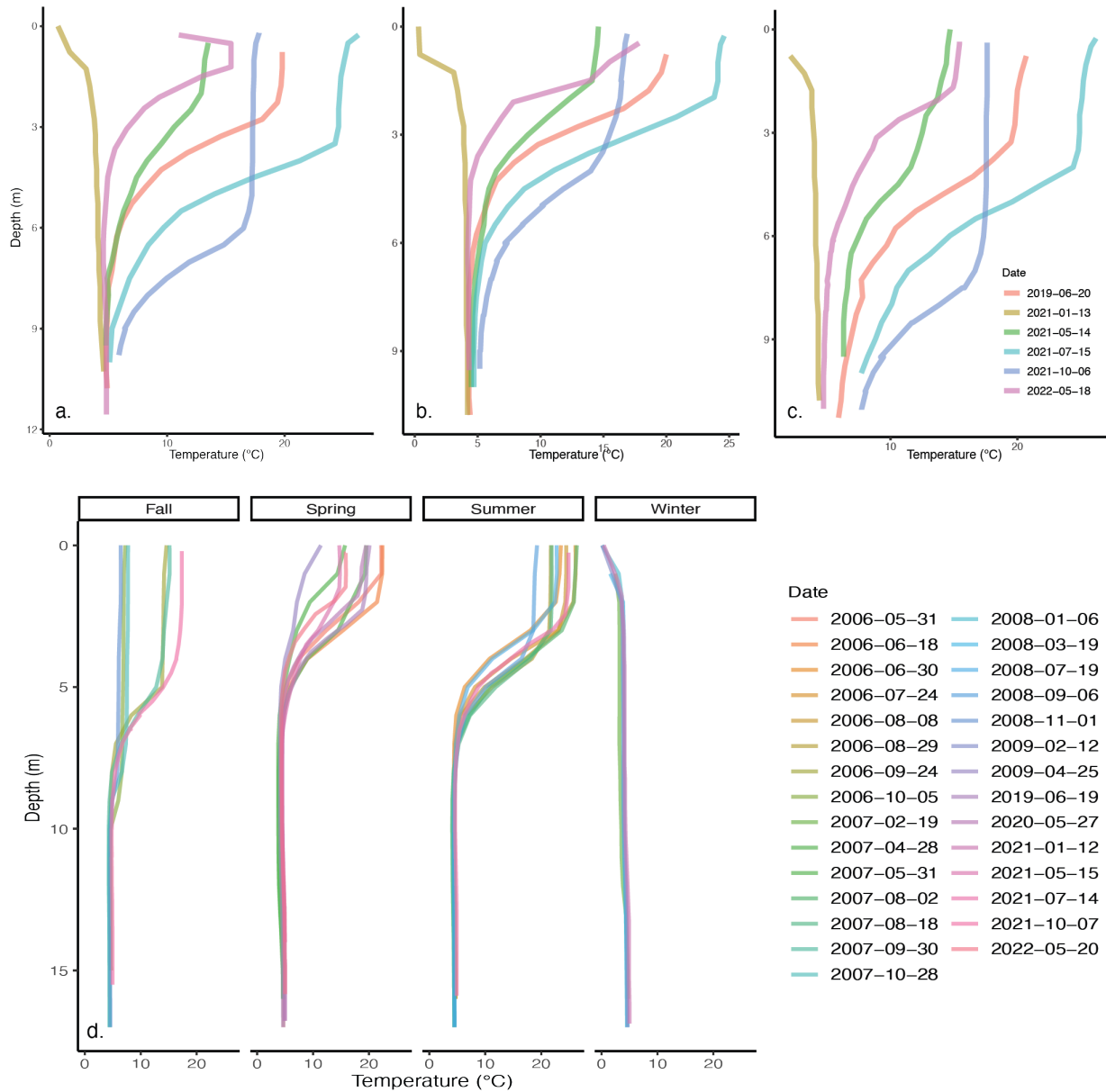
Deming Lake July 14, 2021 Deming Lake October 7, 2022



Supplementary Figure 10. The Brunt-Väisälä or buoyancy frequency (N^2 , s^{-2}), calculated from the temperature and salinity profiles from Deming Lake from January 2021 to May 2022. Higher values indicate greater stability.



Supplementary Figure 11. The Brunt-Väisälä or buoyancy frequency (N^2 , s^{-2}), calculated from the temperature and salinity profiles from Josephine Lake from January 2021 to May 2022. Higher values indicate greater stability.

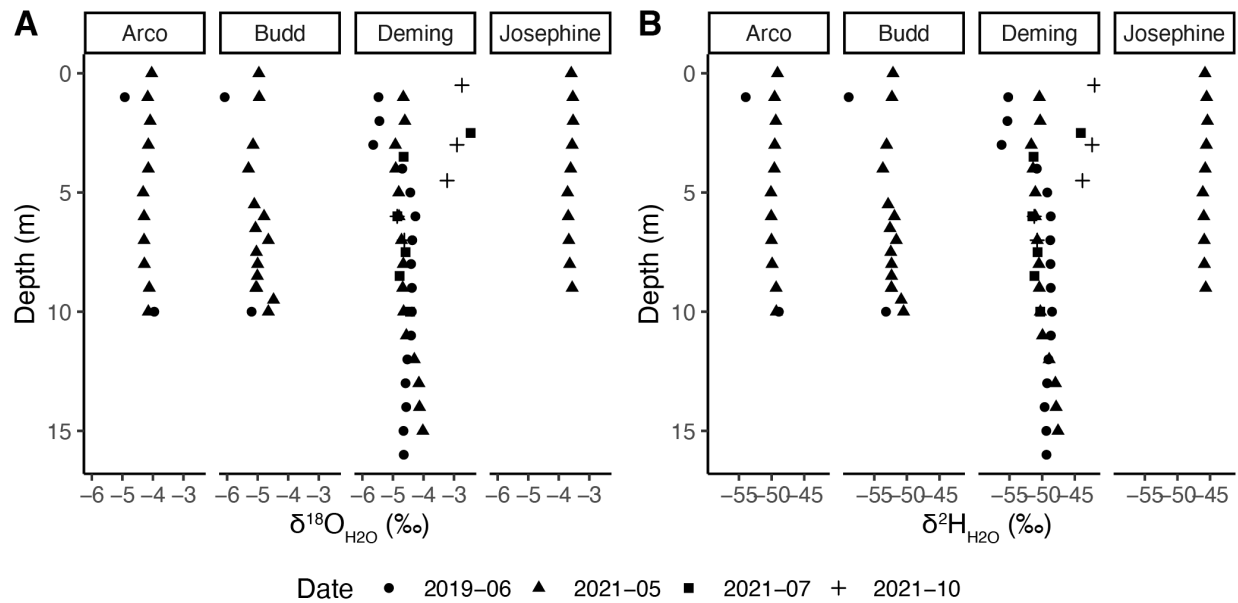


Supplementary Figure 12. Temperature profiles of a) Arco Lake, b) Budd Lake, c) Josephine Lake, and d) Deming Lake. For Deming Lake, seasons were classified according to solstice and equinox dates.

Supplementary Table 1. Water color in mg Pt L⁻¹. The depths of individual samples (in meters) are given in parentheses.

	Arco	Budd	Deming	Josephine
Depth 1	1.4 (4)	32.87 (2)	8.0 (3.5)	3.1 (2)

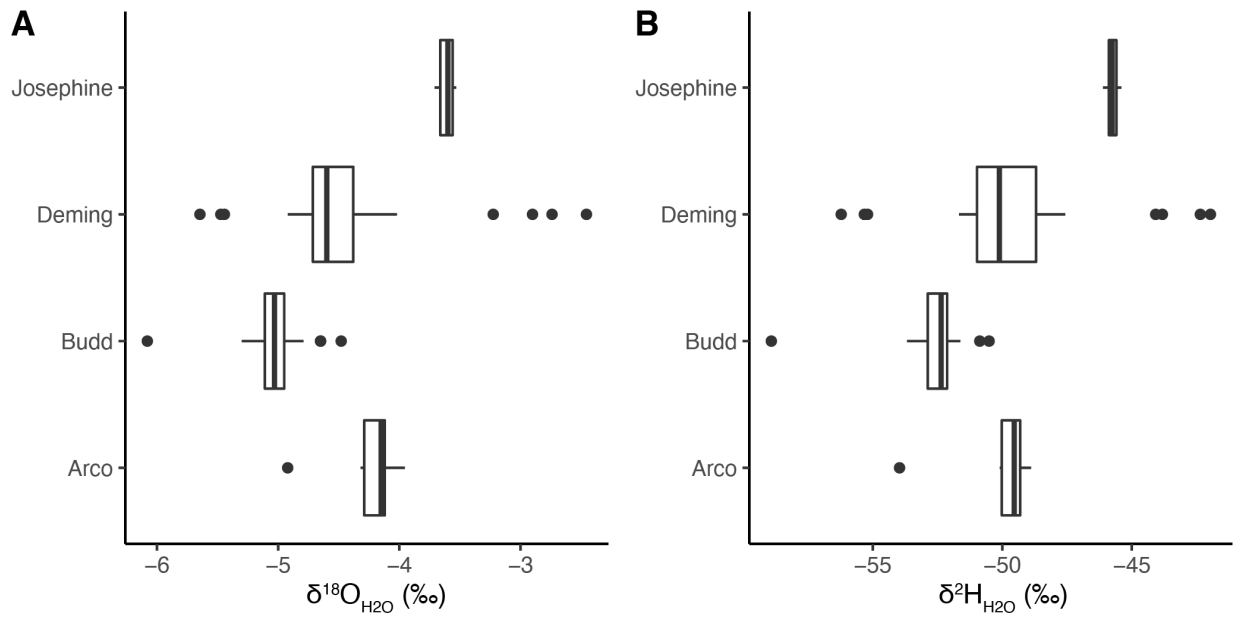
Depth 2	3.1 (5)	27.9 (4.5)	8.0 (4.5)	1.4 (4.5)
Depth 3	4.71 (5.5)	24.6 (9)	8.0 (5)	1.4 (9)
Average	3.1	28.4	8.0	2.0
Standard dev.	1.7	4.2	0	1.0



Supplementary Figure 13. Trends in $\delta^{18}\text{O}_{\text{H}_2\text{O}}$ and $\delta^2\text{H}_{\text{H}_2\text{O}}$ with depth in the four study lakes. Deming was the only lake sampled in all seasons. Analytical precision is within the symbol size.



Supplementary Figure 14. Left: marsh marigold in boggy areas around Deming Lake with 3x4" field notebook for scale. Right: iron mineralization at Elk springs.

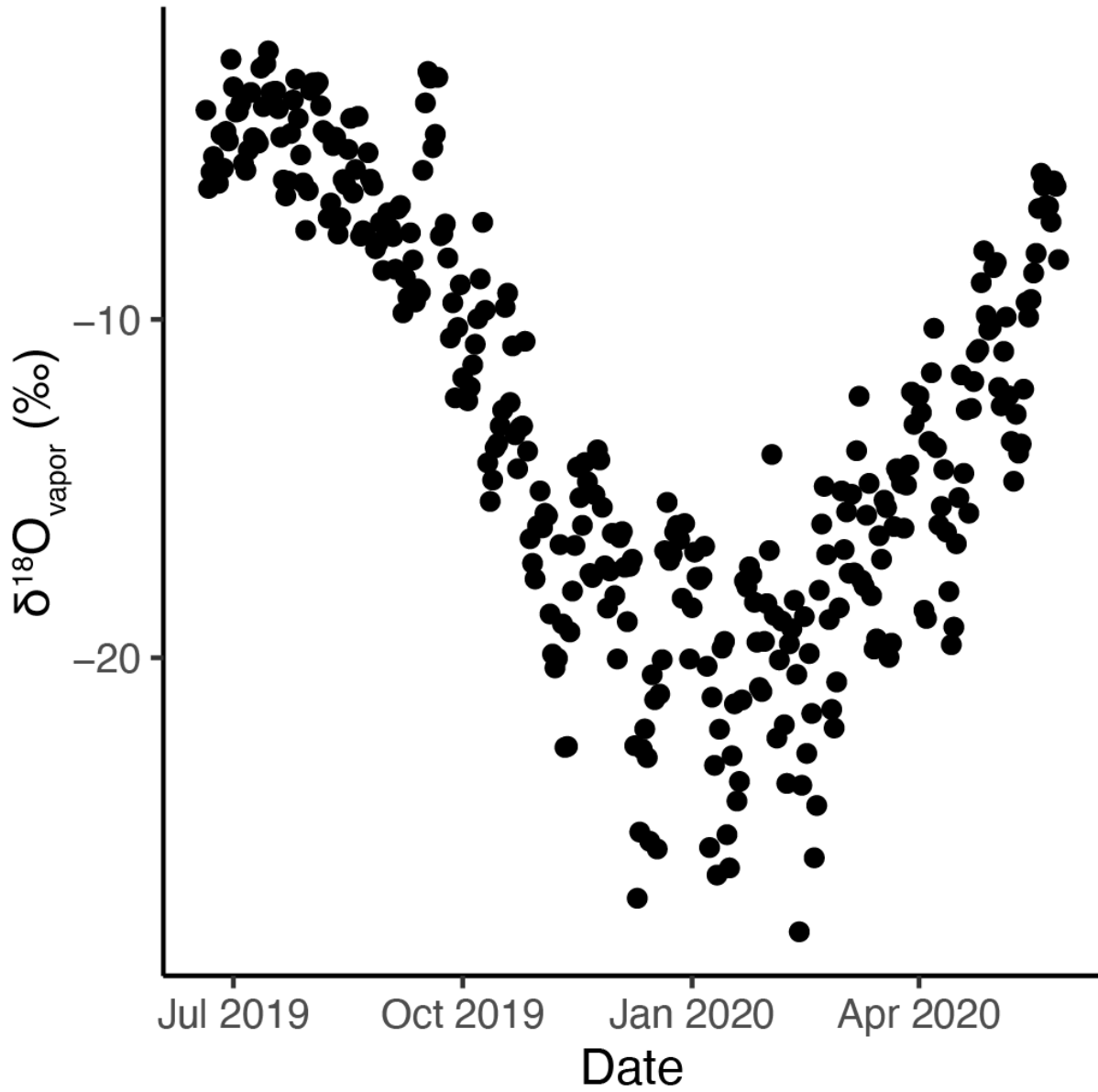


Supplementary Figure 15. The range of $\delta^{18}\text{O}_{\text{H}_2\text{O}}$ and $\delta^2\text{H}_{\text{H}_2\text{O}}$ in the four study lakes for the periods specified in Supplementary Figure 13.

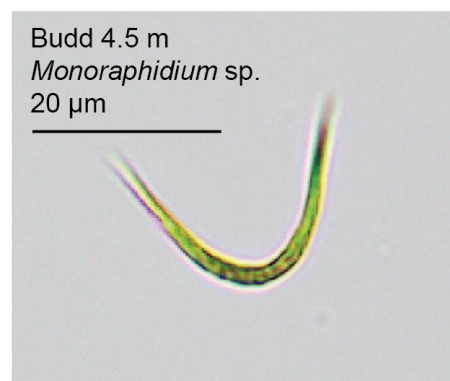
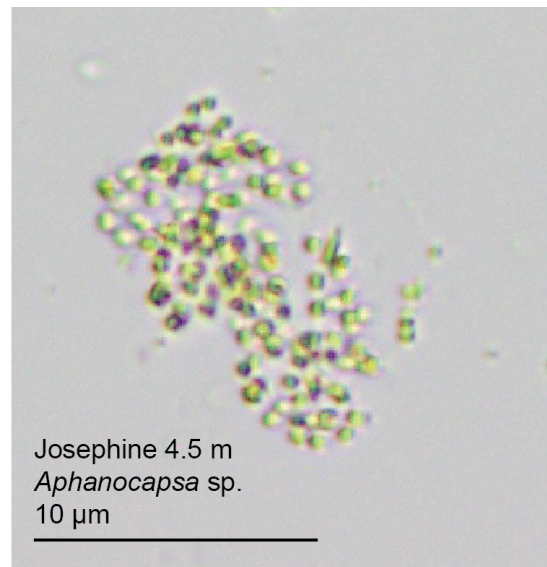
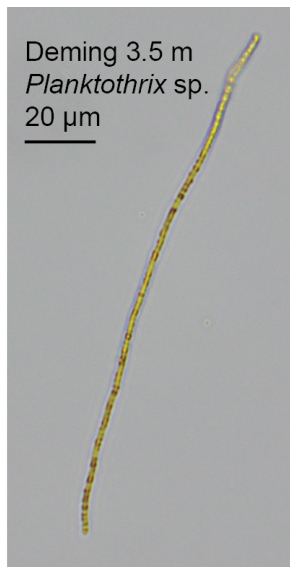
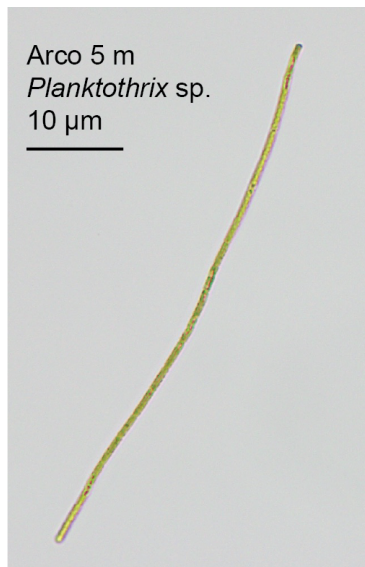
Supplementary Table 2. Stable isotopes of spring and bog water.

Site Name	Latitude	Longitude	$\delta^{18}\text{O}_{\text{H}_2\text{O}}$ (‰)	$\delta^2\text{H}_{\text{H}_2\text{O}}$ (‰)
Deming Bog	47.169440	-95.167162	-6.83	-10.90
Nicollet Creek	47.193874	-95.230539	-10.90	-81.36
Elk3	47.190478	-95.211350	-10.23	-77.36
Elk4	47.190478	-95.211350	-9.34	-73.92

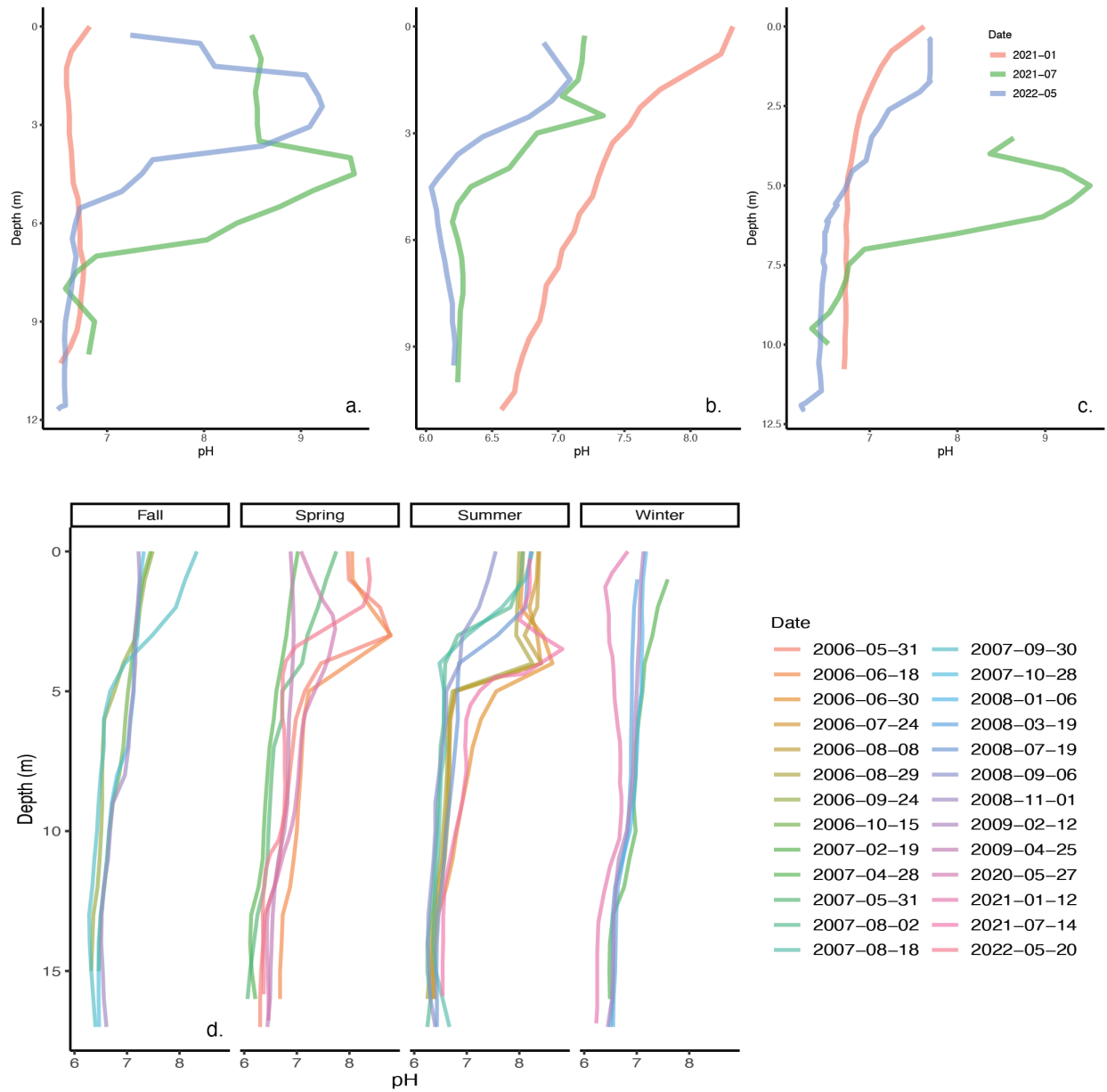
The combined uncertainty (analytical uncertainty and average correction factor) for $\delta^{18}\text{O}$ is $\pm 0.04\text{‰}$ VSMOW) and $\delta^2\text{H}$ is $\pm 0.25\text{‰}$ (VSMOW), respectively.



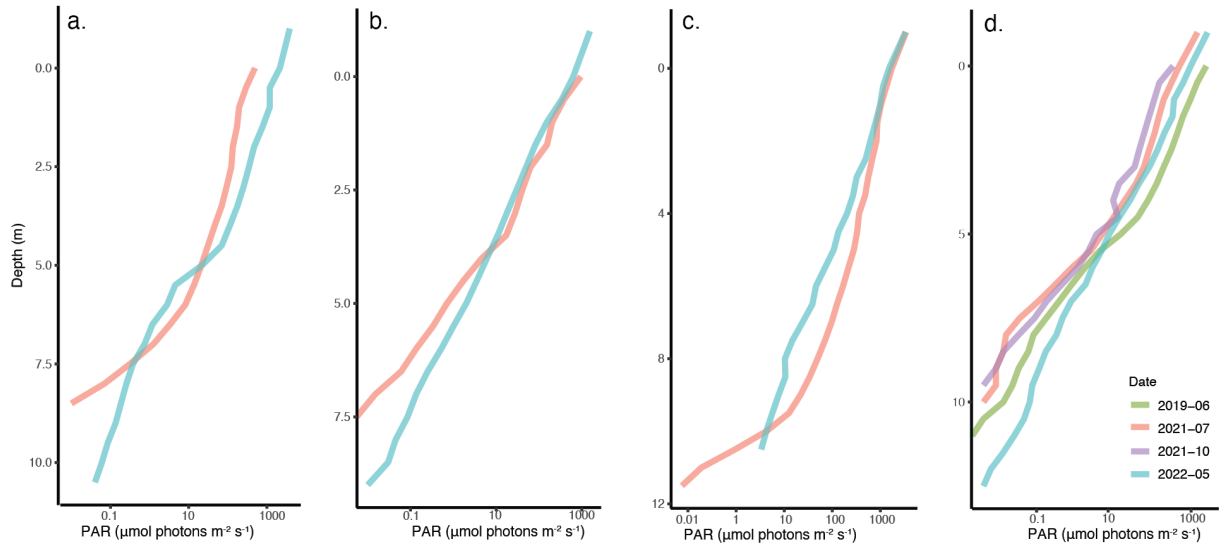
Supplementary Figure 16. The range of $\delta^{18}\text{O}_{\text{H}_2\text{O}}$ calculated for water vapor based on temperature records from the ITCM5 station calculated according to Engel & Magner, 2019.



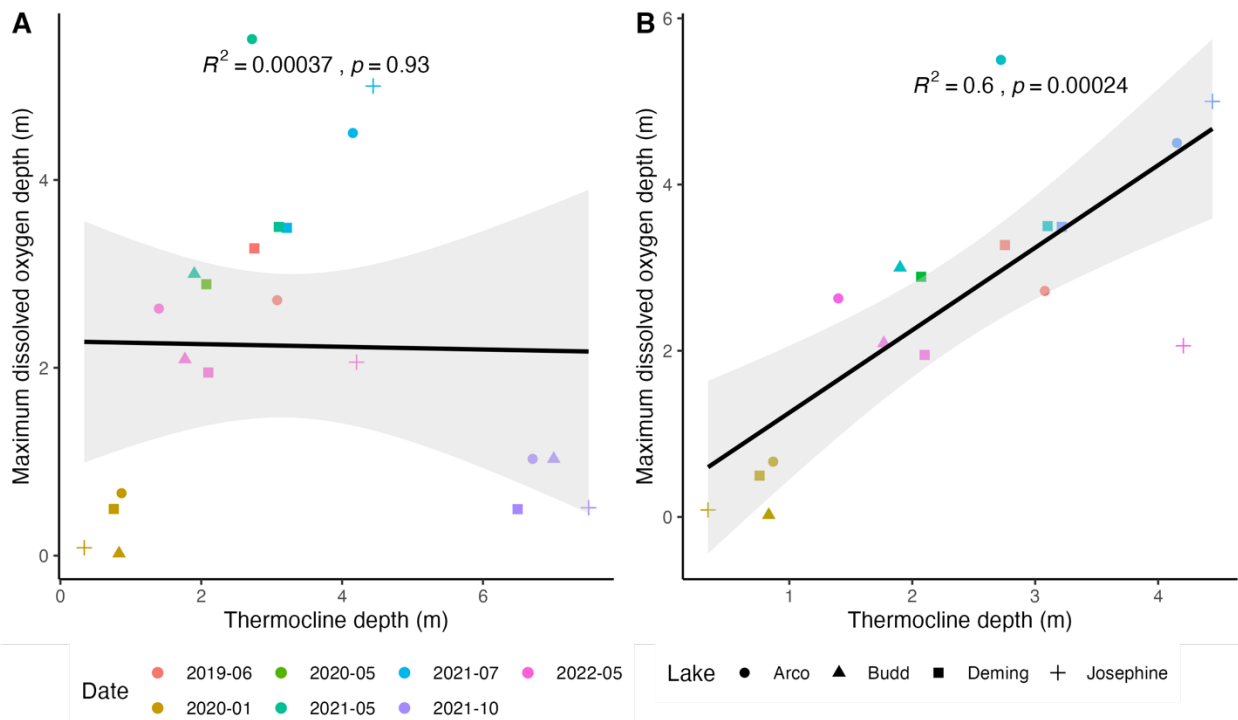
Supplementary Figure 17. Cyanobacteria (top row) and eukaryotic algae (bottom row) observed in the study lakes in May 2022.



Supplementary Figure 18. pH profiles of a) Arco Lake, b) Budd Lake, c) Josephine Lake, and d) Deming Lake. For Deming Lake, seasons were classified according to solstice and equinox dates.



Supplementary Figure 19. Photosynthetically active radiation (PAR) profiles of a) Arco Lake, b) Budd Lake, c) Josephine Lake, and d) Deming Lake.



Supplementary Figure 20. Co-variation between the thermocline depth and the depth of the maximum in dissolved oxygen, and the SCML. Panel A includes data from all dates, and panel B lacks data from October 2021. The correlation is significant when October 2021 datapoints are removed.